

**SPECTRAL CHARACTERIZATION OF SANDY BEACHES
IN WESTERN PORTION OF PUERTO RICO**

By Gretchen M. Chiqués

A thesis in partial fulfillment of the requirements for the degree

MASTER OF SCIENCE
in
GEOLOGY

UNIVERSITY OF PUERTO RICO
MAYAGÜEZ CAMPUS
2005

Approved by:

Wilson Ramírez, Ph. D.
Member, Graduated Committee

Date

Hernan Santos, Ph. D.
Member, Graduate Committee

Date

Fernando Gilbes Santaella, Ph. D.
Chairman, Graduate Committee

Date

Luis Olivieri, MS
Representative of Graduate Studies

Date

Johannes Schellekens, Ph. D.
Chairperson of the Department

Date

Abstract

Remote sensing applications to beach system in Puerto Rico have been limited by low spatial resolution of the available images and lack of appropriate equipment for field validation. A GER-1500 spectroradiometer with a spectral range from 350 to 1050 nanometers was used to collect reflectance measurements in 15 sandy beaches in western Puerto Rico. Samples of the beaches were analyzed in the laboratory to determine the composition using sieving, XRD and grain counting to characterize the different components of the sand sediments. Results indicate a change in magnitude in the reflectance curve compared with the composition. Higher magnitude correlated with more carbonate material concentration in the sand and lower magnitude correlated with higher concentration of dark mineral. The reflectance shows a change in the slope of the reflectance curve between 450 to 550 nanometers that is present in all 15 beaches. The spectral slope in that range was calculated and related to the composition. The results of the field reflectance measurements were compared to high resolution (1m) IKONOS satellite images. Using band math these images showed a correlation with the field measurements. A methodology to obtain information about composition in sand beaches using remote sensing was developed using the slope of the reflectance curve. For the first time a spectral library of beach sand sediment for western Puerto Rico was created.

Resumen

Aplicaciones de Percepción Remota a los sistemas de playa en Puerto Rico han estado limitadas por baja resolución espacial de las imágenes disponibles y la falta de equipo necesario para validar los datos de campo. Un espectroradiómetro GER 1500 fue utilizado para obtener medidas de reflectancia dentro de un rango espectral de 350 -1050 nanómetros en todas las 15 playas arenosas al oeste de Puerto Rico. Muestras de estas playas fueron analizadas en el laboratorio utilizando la técnica de sernir, XRD y conteo de granos para determinar la composición. Los resultados indican que hay un cambio en la pendiente de la curva de reflectancia comparado a la composición. Altas magnitudes se relacionan con más material de carbonato en la arena y bajas magnitudes en la curva de reflectancia se relacionan a altas concentraciones de minerales oscuros. La reflectancia muestra un cambio en la curva entre 450 a 550 nanómetros que esta presente en todas las 15 playas. La pendiente presentada en la curva de reflectancia fue calculada y relacionada a la composición de las arenas. Los resultados de las medidas de reflectancia fueron comparados con imágenes de alta resolución de IKONOS. Una metodología para obtener información sobre la composición en las arenas fue desarrollada utilizando la pendiente de la curva de reflectancia. Por primera vez una librería espectral para los sedimentos de playa en el oeste de Puerto Rico fue creada.

© Copyright by Gretchen M. Chiqués-Torres 2005
All rights reserved

Dedication

*To my beloved husband, my dearest sons and my beautiful baby daughter,
for being always with me,
you are the light of my life,
my inspiration,*

with all my love...

mamá 

Acknowledgments

I would like to give my respects and express my gratitude to all the people that support and help in this project:

- ❖ Dr. Fernando Gilbes, my advisor, for believe in me and being one of pioneer in the application of remote sensing in the coast of Puerto Rico.
- ❖ Dr. Juan Gonzalez, since even start my master you guide me and gave your unconditional support.
- ❖ Doña Iris thanks you for hear all my frustration and help me in everything I need during all my college.
- ❖ Dr. Jack Morelock thanks for all the advice full of experience and wise knowledge.
- ❖ Dr. Wilson Ramirez, thank you so much for all your suggestions and ideas, they help to get a better vision.
- ❖ Dr. Hernan Santos for always been there to help and support me as a student.
- ❖ Angel Cortez for being my friend and for helping in sampling collection and computer performance, you are truly a life saver.
- ❖ Tropical Center for Earth and Space Studies and NASA grant NCC5-518 for providing the necessary support for this research

Table of Content

LIST OF FIGURES.....	viii
LIST OF TABLE	x
Chapter 1: Introduction.....	1
1.1 Objective	2
Chapter 2: Literature Review.....	3
2.1 Geology of the Area	3
2.1.1 North Coast.....	5
2.1.2 West Coast.....	6
2.1.3 South Coast.....	7
Chapter 3: Material and Methods.....	8
3.1 Field Work.....	8
3.2 Laboratory Analyses	14
3.2.1 Sieving	14
3.2.2 X-ray diffractometer.....	15
3.2.3 Grain Counting.....	15
3.3 Laboratory Experiments.....	16
3.4 Digital Processing	18
Chapter 4 : Results.....	21
4.1 Field Measurements.....	21
4.2 Laboratory Analyses.....	21
4.3 Laboratory Experiments.....	33
4.3.1 Carbonate Comparison.....	34
4.3.2 Quartz Comparison	37
4.3.3 Dark Mineral Comparison	39
4.4 Band Ratios Comparison.....	41
4.5 Statistical Analyses.....	47
Chapter 5: Discussion.....	48
Chapter 6: Conclusions.....	52
Chapter 7: Cited Literature.....	54

List of Figures

Figure 1	Beach locations. GIS Geological map of western Puerto Rico from USGS 2001.....	4
Figure 2	Beach locations a) Manatí River Mouth, b) Station 1 from Manatí-Arecibo road 681, c) Station 2 from Manatí-Arecibo road 681 and d) Station 3 from Manatí-Arecibo road 684.....	9
Figure 3	Beach Location a) Guajataca beach b) Jobos beach east, c) Jobos beach west and Crashboat.....	10
Figure 4	Beach location a) Córcega beach, b) El Maní beach, c) Guanajibo River Mouth and El Combate Beach.....	11
Figure 5	Beach location a) El Faro beach, b) Tamarindo beach west and c) Tamarindo beach east.....	12
Figure 6	Sand collections diagram.....	13
Figure 7	Sand of the 15 beaches.....	14
Figure 8	Grain counting matrix. Three hundred grains of each same are classified in one of the five categories listed.....	16
Figure 9	Reflectance curves measured in 15 beaches using the GER-1500 spectroradiometer.	22
Figure 10	Grain count composition for: a) El Faro Beach, b) El Combate Beach, c) Tamarindo west and d) Tamarindo east.	25
Figure 11	Grain size distribution for El Faro Beach, El Combate, Tamarindo west and Tamarindo east.....	26
Figure 12	Grain counting composition for: a) Crashboat, b) Jobos west, c) Sta.3 Manatí- Arecibo and d) Córcega.	28
Figure 13	Grain Size distribution chart for Crashboat, Jobos west, Manati-Arecibo Station 3 and Córcega.....	29
Figure 14	Grain count composition for: a) Guajataca, b) Jobos East, c) El Maní and d) Station #2 Manatí-Arecibo.	30

Figure 15	Grain size chart distribution for Guajataca, Jobos East, El Maní beach and Manati-Arecibo Station 2.....	31
Figure 16	Grain count Composition for: a) Manati River Mouth, b) Station #1 from Manati-Arecibo, c) Guanajibo River Mouth.....	32
Figure 17	Grain size distribution for Manatí River Mouth, Station #1 from Manatí- Arecibo and Guanajibo River Mouth.....	33
Figure 18	Carbonate material in this samples are from El Faro Beach.....	35
Figure 19	Carbonate material in these samples is from Playa Tamarindo.....	35
Figure 20	Carbonate Comparison with the two sources of carbonated material.....	36
Figure 21	El Faro Beach carbonate source quartz comparison	37
Figure 22	Tamarindo carbonate source quartz comparison	38
Figure 23	Quartz comparisons between the El Faro Beach carbonate materials source and Tamarindo beach source.	38
Figure 24	El Faro Beach carbonate source for dark mineral model.....	39
Figure 25	Tamarindo beach carbonate source for dark mineral model.....	40
Figure 26	Dark Mineral comparison between El Faro Beach and Tamarindo carbonate source.....	40
Figure 27	Example of IKONOS band math. The beach is Crashboat, Aguadilla. Band ratios B1/B2, B4/B3 correlates with GER data. Last image is B3/B2.....	42
Figure 28	Band Ratio comparison between GER 1500 and IKONOS. a) El Faro Beach, b) El Combate, c) Tamarindo west and d) Tamarindo east	43
Figure 29	Band Ratio comparison between GER 1500 and IKONOS. a) Crashboat, b) Jobos West, c) Manatí-Arecibo 3 and d) Córcega	44
Figure 30	Band Ratio comparison between GER 1500 and IKONOS. a) Guajataca, b) Jobos East, c) El Maní and d) Manatí-Arecibo 2.....	45
Figure 31	Band Ratio comparison between GER 1500 and IKONOS. a) Manatí River Mouth, b) Manatí-Arecibo 1, and c) Guanajibo	46

List of Tables

Table 1	Beach Sampling location (datum State Plane NAD 83 and WGS 84).....	13
Table 2	Udden-Wentworth grain size scale.....	15
Table 3	Experiment Samples ID and Composition distribution in percentage of mineral groups.....	17
Table 4	Experiment Sample ID and Composition distribution in percentage of mineral groups	18
Table 5	Spectral slope in the range of 450 -570 nm for the 15 beaches.....	23
Table 6	T-test for paired results.....	47

Chapter 1

Introduction

The coastal zone of Puerto Rico is remarkably diverse. Unlike the shorelines of major continents, there are no long interrupted stretches of uniform beach. The beaches of Puerto Rico are relatively short and are divided into separate systems that have restricted communication with each other. Each one is a closed or semi-closed unit receiving its supply of sediments from limited local sources and transmitting little of its long shore moving sand to another beach system (Morelock, 2000).

Sand sediment grains size helps to determine current force transport. Sand sediment composition provides important clues about the source of origin of the individual grains (Morelock, 1978). The sources of beach sand in Puerto Rico are relatively limited. These include;

Offshore sands - moderate erosion residue, relict Pleistocene deposits from rivers and estuaries.

Erosion of land - alluvial river valleys, cliff erosion alluvial or rock, eolianites and beach rock.

Biogenic material – shell accumulations from coral reefs.

Previous studies of Puerto Rico beaches have measured sand sediment composition, profiles of the beach and sediment transport, but only a few of them have used remote sensing. The main reasons for these minimum applications of remote sensing to beach system in Puerto Rico have been the low spatial resolution in available images and lack of appropriate equipment for field validation. However, the new technology allows us better studies for sediment characterization. For example, with the GER 1500 spectroradiometer is possible to get the reflectance (a measurement of how much electromagnetic radiation is reflected out of a surface) of beach sand. These data integrated with satellite imagery of high spatial resolution give new tools for monitoring beach sand sediment composition and specific characteristics in grain size distribution. For a naked eye the grains composition of the sand is correlated with its color. Usually

dark color sand is related to higher terrigenous material concentration. Beige color sand is associated to a mixture of grain like carbonates, quartz and igneous rock fragment. White color sand is associated to homogeneous composition of carbonate material or quartz (Morelock, 2000). Based on this, it is expected that differences in the reflectance curve (produced by the differences in color) will be related with the composition of the sand.

In order to test this hypothesis, we determine the relation of the texture and the composition of the sand with its reflectance curve. Also, a spectral library was produced for future studies. The data will help in future monitoring of beaches, allowing rapid analyses of beach sand composition.

There are several beach systems in the northwest, west and southwest part of the island with differences in composition and texture of sands. Specific beaches that were examined in this study included: Barceloneta, Arecibo, Aguadilla, Añasco, Guanajibo, Cabo Rojo and Caña Gorda. Each site has a unique sediment composition and different source for the beach sands.

1.1 Objectives

Preliminary studies recently made in western beaches of Puerto Rico showed a possible relationship between reflectance and sand texture and composition (unpublished undergraduate research). These observations suggest that spectral information could be use to remotely determine the texture and composition of beaches without the need of field work. Based on this hypothesis, the main objectives of this study are:

- Develop a database of the reflectance curves for several types of the sandy beaches for the west coast of Puerto Rico.
- Create a spectral library for each beach for future reference.
- Determine how texture and composition affects the shape and magnitude of the reflectance curve of beach sand.
- Compare the developed spectral library with satellite images.
- Develop a remote sensing technique to characterize differences of beach sand composition and texture of beaches around Puerto Rico.

Chapter 2

Literature Review

In 1959, Kaye wrote about the changes of shoreline features and how the geology determines the type of beach. Morelock (1978) described the coastal types of Puerto Rico and the sediment transport along beaches. In 1997, Barreto studied the sediment budget of the shoreline in Puerto Rico applying remote sensing techniques available at that time.

These works describe sand composition in different beaches of Puerto Rico, but only the last one used remote sensing. At that moment the available technology was limited and remote sensing was used for mapping the changes in the coast line through time. However, the composition or the characteristics of the sediment were not studied using this technique.

A preliminary research done by Cameron (un-published undergraduate research, 2003) determined the reflectance curves of the sand of four beaches along western Puerto Rico. The four beaches had different sand composition. He found a relationship in the magnitude of the reflectance curve and the composition of the sand.

2.1 Geology of the Study Area

This study considered beaches from Barceloneta at the river mouth of Rio Grande de Manatí through the west to Aguadilla, from Aguadilla to Cabo Rojo, and from Cabo Rojo to Caña Gorda in Guánica show in Figure 1. These coastal areas show different sand composition and grain size. Morelock in 1978 described the beaches around Puerto Rico as follow.

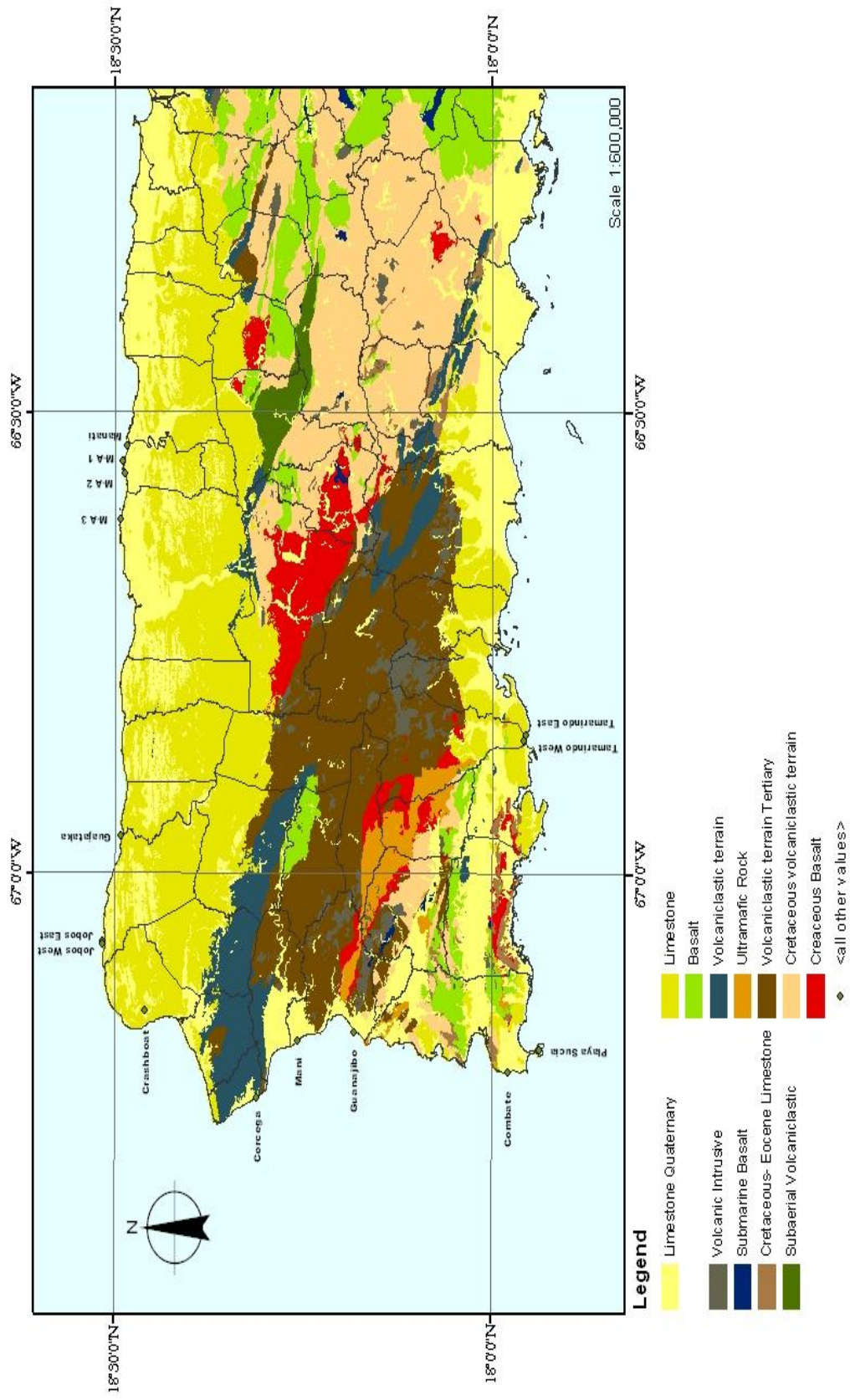


Figure 1: Geological map of central and western Puerto Rico from USGS 2001

2.1.1 North Coast

The north coast, from Arecibo to Aguadilla, has a series of rocky cliffs with sandy beaches and dunes between them. The prominent features are the high hills in the interior and high cliffs along the coast, where low coastal plains with beaches are present, although they are less than a kilometer width. The selected areas for this study between Manatí to Aguadilla are Barceloneta, Arecibo, Guajataca and Isabela.

Barceloneta - The Manatí River carries large amounts of igneous rock material, dark minerals and magnetite. These minerals dominate the beaches to the west of the river mouth. There is a slow decrease in these minerals and an increase in carbonate material toward Jarealito.

Arecibo - The beach is dominantly composed by carbonate grains with some igneous rock fragments between Tres Hermanos and Jarealito. In the west of Rio Arecibo, the beach has quartz, light minerals and igneous rock fragments in roughly equal portions. Some of the beaches (Arecibo, Quebrada Seca West) show a very high content of magnetite. Both the Arecibo and Camuy rivers contributed sediments into the beach system. In about half of the coastal areas the limestone bluff is several hundred meters to several kilometers from the shoreline, and it is a beach plain. After heavy flooding, the magnetite content in the beach increases due to new sediment from the central mountain (Morelock, personal communication).

Guajataca - This beach has quartz, light minerals, and igneous rock material carried to the area by the Rio Guajataca. It is isolated from the other beaches by rocky headlands.

Isabela - West of Jobos Beach, there is a short stretch of coast that is primary, resulting from sub aerial deposition by wind, and is a dune coastline. Its main composition is carbonated sand.

2.1.2 West Coast

The structural mountains dominated the coast from Aguadilla to Cabo Rojo, the coast is dominated by the effect of structural mountain ridges separated by broad alluvial valleys. The ridges form a rocky coast and sandy beaches occupy the shoreline bordering the alluvial valleys (Morelock, 1978). The selected areas from Aguadilla to Cabo Rojo are Aguadilla, Añasco, Guanajibo and Cabo Rojo.

Aguadilla - Punta Borinquen and Crashboat beaches are isolated bounded by rocky shoreline. The beach is continuous from Aguadilla to Punta Gorda, and it is a beach plain. The beach sediments are composed of approximately equal parts of carbonate shell material, quartz and light minerals, and igneous rock fragments. Rio Culebrinas and Rio Grande carry sediments from a large drainage basin to this part of the coast.

Añasco - The Córcega beach sands are composed of carbonate, quartz, and igneous rock fragments with minor amounts of light minerals. It is a fairly broad beach with a steep foreshore face. The beach terminates at Punta Cadena, with a rocky shoreline. The carbonate content decreases southward until it reaches the Maní Beach, where the dominant component is igneous rock fragments with quartz, and light minerals and some carbonate grains.

Guanajibo - Mayagüez Beach is composed of igneous rock fragments, magnetite, other dark mineral grains, and minor amounts of light minerals grains. The mineralogy is very different from the Añasco Beach system. The canyon at the Mayagüez Harbor entrance blocks the transport of sand from the Añasco system to the Mayagüez Beach.

Cabo Rojo - El Combate beach is composed of quartz and calcium carbonate sand. El Faro beach composed of carbonate and quartz has a unique circulation patterns in the bay between Cabo Rojo and Punta Molino. As the surface currents move westward along the south coast of Puerto Rico, part of the flow passes Cabo Rojo and continues into the Mona Passage. Part of the flow is diverted into the

bay and carries surface debris to El Faro Beach. The bay contains large quantities of sand, which moved southwest and cross Cabo Rojo (Morelock, 1978).

2.1.3 Southwest Coast

The southwest coast is very irregular, with projecting brush covered points of limestone between shallow coves and bays. Except for the eastern and western ends of the south coast and the Guánica area, the land is low near the shore. The shoreline development is related to the adjacent land area of the coast (Cretaceous-Tertiary limestone, igneous rock, early Tertiary sediment fans, or alluvial plains). The limestone outcrops form a rocky coast with small local sand or gravel beaches. In many places, the growth of mangrove altered the shoreline. (Morelock, 1978). The selected beach for this area is Tamarindo Beach (east of Caña Gorda).

Caña Gorda - There is no evidence of communication and passage of sand from one beach to another. Offshore carbonate inputs and calcium carbonate grains derived from erosion of the limestone cliffs compose these beaches, One of the largest is Caña Gorda, composed of calcium carbonate sands. (Morelock, 1978).

Chapter 3

Material and Methods

3.1 Field Work

The fifteen (15) beaches selected of the western part of Puerto Rico (Figures from 2,3,4 and 5):

- Manatí River mouth, Barceloneta
- Road #681 from Manatí to Arecibo Sta. 1
- Road #681 from Manatí to Arecibo Sta. 2
- Road #684 from Manatí to Arecibo Sta. 3
- Guajataca beach, Quebradillas
- Jobos beach, Isabela, east side and west side.
- Crashboat, Aguadilla
- Córcega beach, Rincón
- El Maní beach, Mayagüez
- Guanajibo River mouth
- El Combate beach, Cabo Rojo
- El Faro beach, Cabo Rojo
- Playa Tamarindo, Guánica, east side and west side.

Three samples for each beach were collected at three different places, with a 12-meter horizontal spacing between and parallel to the beach along the dry zone (Figure 6). Specific locations were registered in each beach using a GPS. The points were recorded in North American Datum State Plane NAD 83 and WGS 84 (Table 1).

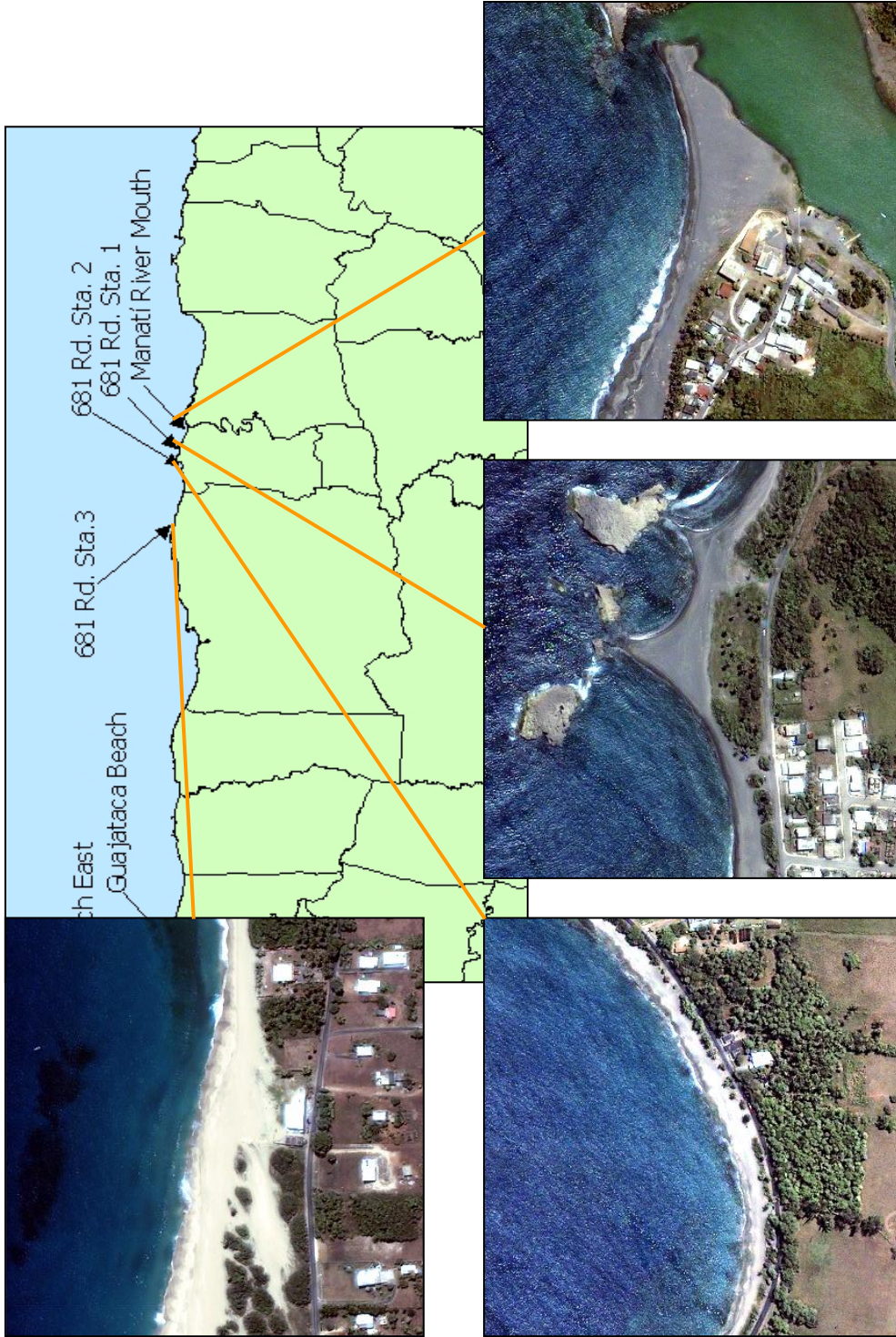


Figure 2: Beach locations a) Manatí River Mouth, b) Station 1 from Manatí-Arecibo road 681, c) Station 2 from Manatí-Arecibo road 681 and d) Station 3 from Manatí-Arecibo road 684



Figure 3: Beach Location a) Guajataca beach b) Jobs beach west and Crashboat. c) Jobs beach east, d) Guajataca beach

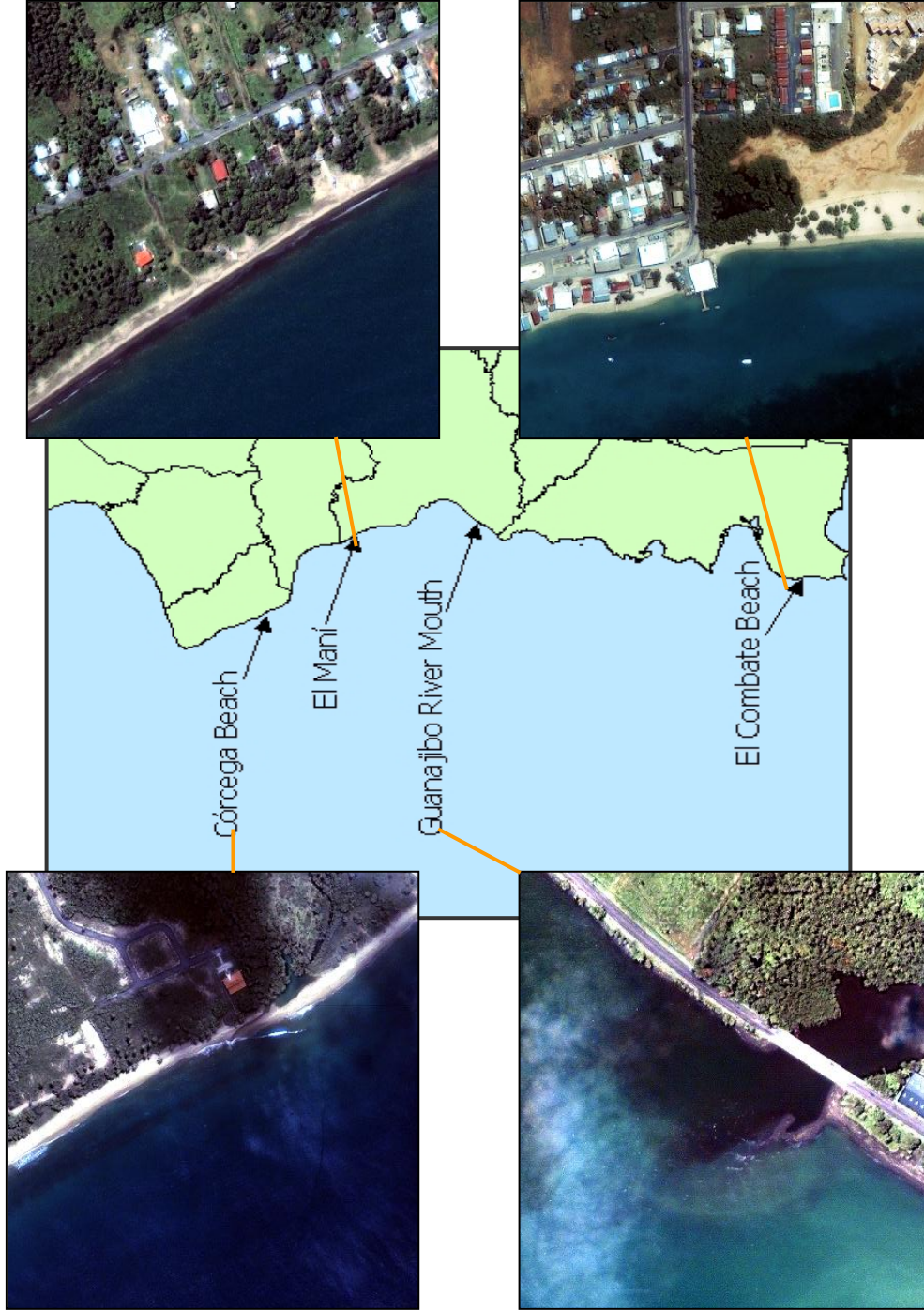


Figure 4: Beach location a) Córcega beach, b) El Maní beach, c) Guanajibo River Mouth and El Combate Beach

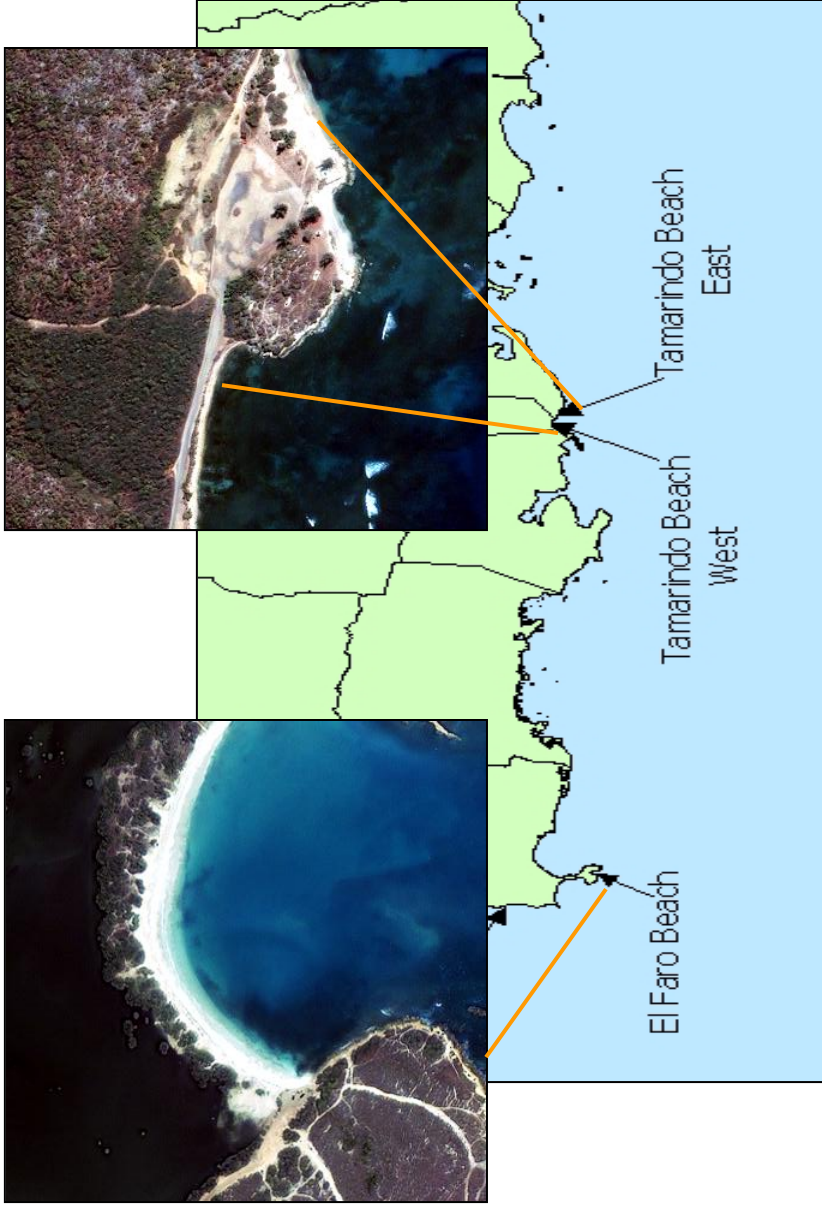


Figure 5: Beach location a) El Faro beach, b) Tamarindo beach west and c) Tamarindo beach east



Figure 6: Sand collections diagram. Each dot represent where sand was collected.

Table 1: Beach sampling locations (datum State Plane NAD 83 and WGS 84).

Location	Northing	Easting	Latitude	Longitude
Manatí River Mouth	271933.34	189292.97	18° 28' 58.57	66° 32' 59.57
Road #681 Station 1	272659.77	187515.00	18° 29' 23.16	66° 33' 05.58
Road #681 Station 2	272406.18	186071.52	18° 29' 14.88	66° 33' 54.78
Road #684 Station 3	273037.61	180868.12	18° 29' 35.08	66° 36' 52.57
Guajataca Beach	272903.28	144493.16	18° 29' 28.62	66° 57' 32.13
Jobos Beach East	275714.69	132429.19	18° 30' 58.81	67° 04' 23.70
Jobos Beach West	275713.74	132165.02	18° 30' 58.75	67° 04' 32.71
Crashboat	269546.29	124504.16	18° 27' 37.24	67° 09' 53.07
Córcega Beach	253126.86	114572.49	18° 18' 41.86	67° 14' 29.09
El Maní	247005.16	121051.07	18° 15' 23.65	67° 10' 47.62
Guanajibo River Mouth	238832.73	121972.76	18° 10' 57.96	67° 10' 15.13
El Combate Beach	216251.29	117402.18	17° 58' 43.26	67° 12' 47.38
El Faro Beach	211538.05	119878.43	17° 56' 09.90	67° 11' 22.55
Tamarindo Beach East	213513.74	156032.05	17° 57' 17.93	66° 50' 54.20
Tamarindo Beach West	213888.66	155373.89	17° 57' 30.07	66° 51' 16.60



Figure 7: Sand of the 15 beaches, the order corresponds to the magnitude of the measurement with the GER 1500 from high (left) to low (right).

Spectroradiometer GER 1500 collected reflectance measurement at every location in the dry sand zone.. The instrument has 512 channels with a spectral range from 350 to 1050 nm (visible to near infrared). It measures the radiance (a measurement of the light reflected by the surface of the object) and the irradiance (a measurement of the incoming sunlight). These measurements have to be converted from radiance to reflectance using this equation:

$$\text{Reflectance} = \frac{L_{\text{object}}}{(L_{\text{card}})^2} \quad (1)$$

Where:

L_{object} = Radiance from the sand

L_{card} = Radiance from a standard gray card. The card used in this study reflected 50% of sun light.

3.2 Laboratory Analyses

3.2.1 Sieving

To determine the grain size distribution (granulometry) we used sediment sieving, a nest set of sieves placed from the size of the mesh progressively smaller down the stack. The sizes of the mesh in this study went from 2 mm (very coarse sand) to 0.0625 mm (very fine sand), measured approximately every 0.50 mm interval. The methodology is described by Folk (1980). We divided the sand with a sand splitter, collecting approximately 500 grams of sand and presented the results in phi (Φ). One phi unit is

equal to one Udden-Wentworth grade. To compute the phi diameter, take the negative log of the diameter in millimeters. The mesh measures for this study are in Table 2.

Table 2: Udden-Wentworth grain size scale

Φ	mm
-1	2mm
-0.75	1.75mm
-0.25	1.25mm
0	1.00mm
1	0.50mm
1.25	0.40mm
1.5	0.35mm
2	0.26mm
2.5	0.180mm
3	0.120mm
3.5	0.09mm
4	0.0625mm

3.2.2 X-ray diffractometer (XRD)

The X-ray diffractometer allows the determination principal minerals in the sample. The X-rays diffractometer D-5000 from Siemem was used to determine each specific compound. The sand was pulverize and used to fill the plates used for the instrument to analyze the sand. The D-5000 is completely computer-controlled for data acquisition. For the phase identification we used the automated search/match software and CD-ROM library of mineral identification.

3.2.3 Grain counting

Grain counting determined the composition of the sand by counting three hundred grains of every sample and classified in one of these five categories base on the minerals founded in the XRD analyzes:

- a) Carbonate – white or very light grain, these grains are identified with hydrochloric acid. The acid dissolves carbonate grains. Carbonated minerals found included calcite, magnesium calcite, aragonite and dolomite.
- b) Quartz – Grains are transparent, colorless. The only component mineral under this category is quartz.
- c) Light minerals – light-medium color grains include quartz, albite and anortite
- d) Dark Minerals – dark color grains, this includes augite and andradite.
- e) Magnetite- usually fine dark metallic grains

1	2	3	4	5	6	7	8	9	10
11	12	13	14	15	16	17	18	19	20
21	22	23	24	25	26	27	28	29	30
31	32	33	34	35	36	37	38	39	40
41	42	43	44	45	46	47	48	49	50
51	52	53	54	55	56	57	58	59	60
61	62	63	64	65	66	67	68	69	70
71	72	73	74	75	76	77	78	79	80
81	82	83	84	85	86	87	88	89	90
91	92	93	94	95	96	97	98	99	100

Figure 8: Grain counting matrix. Three hundred grains of each same are classified in one of the five categories listed.

We calculated the percentage after the classification for each category. This analysis determined the composition of each individual grain and the estimated frequency of variable constituents in the sediment sample.

3.3 Laboratory Experiments

After sieving the sand from the 15 beaches, we obtained a standard sample grain size of 2.0Φ of each category (carbonate, quartz, light minerals, dark mineral) and 3Φ

grains size of magnetite. We mix the sand, creating different sand mixtures with controlled compositional distribution (Table 3 and Table 4). Each sample of the modeling consists of a total of 10 ml volume for each mixture.

Measurements taken with the GER-1500 collected the changes of the reflectance curve under controlled composition mixture.

Calculations of the slope of the reflectance curve determine if there is any correlation between the slope of the curve and the composition of the sand.

Table 3: Experiment Samples ID and Composition distribution in percentage of mineral groups. Carbonates of these samples are from skeletal source.

Sample ID	Carbonate	Dark Mineral	Light Minerals	Magnetite	Quartz	Slope
TM-1	100	-	-	-	-	0.0016
TM-2	90	10	-	-	-	0.0014
TM-3	80	20	-	-	-	0.0014
TM-4	70	20	10	-	-	0.0013
TM-5	60	20	20	-	-	0.0015
TM-6	50	20	20	-	10	0.0014
TM-7	40	20	20	10	10	0.0009
TM-2D	10	60	30	-	-	0.0008
TM-3D	10	50	40	-	-	0.0010
TM-4D	10	40	40	10	-	0.0011
TM-5D	10	30	50	10	-	0.0009
TM-6D	10	20	50	10	10	0.0010
TM-1Q	40	-	-	-	60	0.0020
TM-2Q	50	-	-	-	50	0.0016
TM-3Q	50	-	10	-	40	0.0018
TM-4Q	40	-	20	-	40	0.0019
TM-5Q	30	20	20	-	30	0.0012
Round	100	-	-	-	-	0.0014
DK	-	100	-	-	-	0.0004
Light minerals	-	-	100	-	-	0.0012
Magnetite	-	-	-	100	-	9E - 05
Quartz	-	-	-	-	100	0.0020

Table 4: Modeling Sample ID and Composition distribution in percentage of mineral groups. Carbonates on these samples are from outcrop erosion.

Sample ID	Carbonate	Dark Mineral	Light minerals	Magnetite	Quartz	Slope
El Faro Beach 1.5Φ	100	-	-	-	-	0.0017
PM-1	100	-	-	-	-	0.0023
PM-2	90	10	-	-	-	0.0015
PM-3	80	20	-	-	-	0.0014
PM-4	70	20	10	-	-	0.0013
PM-5	60	20	20	-	-	0.0016
PM-6	50	20	20	-	10	0.0012
PM-7	40	20	20	10	10	0.0013
PM-1D	-	70	30	-	-	0.0012
PM-2D	10	60	30	-	-	0.0009
PM-3D	10	50	40	-	-	0.0010
PM-4D	10	40	40	10	-	0.0008
PM-5D	10	30	50	10	-	0.0010
PM-6D	10	20	50	10	10	0.0010
PM-1Q	40	-	-	-	60	0.0019
PM-3Q	50	-	10	-	40	0.0019
PM-4Q	40	-	20	-	40	0.0018
PM-5Q	30	20	20	-	30	0.0011

3.4 Digital Processing

IKONOS satellite images were compared to the field data measured by the GER-1500.

The IKONOS images used in this study are from the dataset of the island requested by the Government of Puerto Rico and are from January to July between 2001 and 2002. These images had four bands, including three in the visible and one in the near infrared. The images had 1 meter spatial resolution provided by Space Imaging. Images

were radiometric calibrated to convert the digital values to radiance measurements using equation (2).

$$Radiance = \frac{DN}{CalCoef} \quad (2)$$

Where:

DN = image product digital values
CalCoef= In-band Radiance Calibration Coefficient
(Values obtained in Spaceimaging.com)

ENVI software (version 3.6) was used for all image processing. Since the specific dates of the images were not available, dark pixel subtract method was used for the atmospheric correction. Band ratios calculated with equation (3) were used to compare the satellite images and the field measurements collected by the GER-1500 spectroradiometer. Band ratios are better for these comparisons because it eliminates the problem of units.

$$Band\ Ratio = \frac{B_x}{B_y} \quad (3)$$

Where:

$B_x / B_y = B$ for band, x or y any band available

The corresponding spectral ranges for the bands used in this study are:

- Band 1 (blue): 0.45 -0.52 μm
- Band 2 (green): 0.51 – 0.60 μm
- Band 3 (red): 0.63 – 0.70 μm
- Band 4 (IR): 0.76-0.85 μm

Two tail paired t-test was used to correlate band ratio from the GER-1500 and the IKONOS images. Paired-sample t-testing require that each datum in one sample is correlated with one datum in another sample (e.g. GER-1500 datd and IKONOS data).

This test used the difference within each pair of measurement. The null hypothesis (H_0) in this test is that there is no difference between pair [$t \leq t_{0.01}$] and the alternate hypothesis (H_a) is there is a difference between pair [$t > t_{0.01}$] with a confidence level of α (0.01).

The statistic test for the null hypothesis is

$$t = \frac{\bar{d}}{S_{\bar{d}}} \quad (4)$$

Where:

\bar{d} = mean of the differences or the error between GER-1500 and IKONOS

$S_{\bar{d}}$ = standard error (root square of the standard deviation of the difference or error)

Spectral slope was calculated in Microsoft EXCEL software. A trend line was calculated for values between 450 to 550 nanometer. The equation was display and the values of the slope obtained from the equation:

$$y = mx + b \quad (5)$$

Where:

y = y axis

m = slope value

x = x axis

b = intercept in y

Chapter 4

Results

4.1 Field Measurements

Reflectance measurements collected with the GER-1500 spectroradiometer are shown in Figure 9. Data obtained from the laboratory analysis (sieve and grain counting) was used to compare the 15 beaches.

The differences in curves magnitude correlated very well with the composition of the beach. Higher magnitude values correlated with higher carbonate content (>50%). Lower magnitude values correlated with higher dark mineral content (>50%). Intermediate values correlated with light minerals mineral contents (30% - 50%). Grain size does not affect the reflectance as much as the composition, but finer grains tended to increase the magnitude value in beaches with same mineral composition. Few data was obtained to validate the impact of grain size over the reflectance curve.

Another characteristic affecting the magnitude of the reflectance curve was the type of carbonate mineral. Beaches with high carbonate content showed differences in the magnitude of the values (discussed in section 4.2). Calculations of the spectral slope (between 440 and 570 nanometers) in the reflectance curve (Table 5) shows that steep slope correlates with high concentration of carbonate and quartz and gentle slope correlated with high dark mineral content.

4.2 Laboratory analyzes

Grain count of every beach shows a correlation between the composition of the sand and the magnitude of the reflectance curve. El Faro Beach had the highest reflectance with 80% of carbonate material and 10% of quartz (Figure 10). El Combate had the highest quartz content with 61% and only 35% of carbonated material. Tamarindo west and Tamarindo east had the highest carbonated component with 96% and 95%, respectively. In the reflectance curve, these last two beaches had lower magnitude than El Faro Beach.

Reflectance Curves

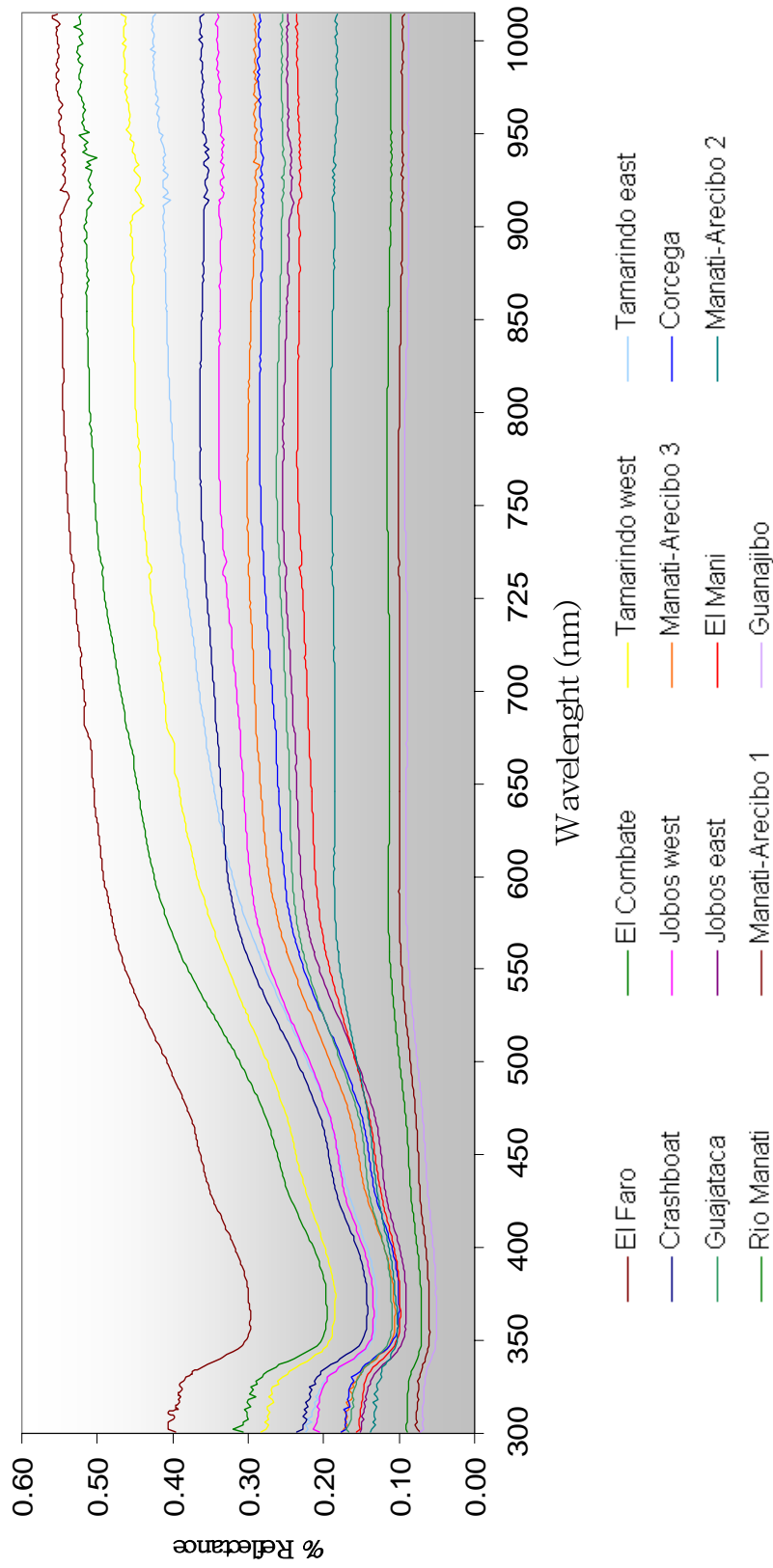


Figure 9: Reflectance curves as measured in 15 beaches using the GER-1500 spectroradiometer. The order of the legend (from left to right) corresponds to the magnitude in the reflectance.

Table 5: Spectral slope in the range of 450 -570 nm for the 15 beaches

Beach	Slope
El Faro Beach	0.0017
El Combate Beach	0.0022
Tamarindo west	0.0017
Tamarindo east	0.0017
Crashboat	0.0019
Jobos west	0.0016
Manatí -Arecibo Road #684 Station 3	0.0016
Córcega Beach	0.0016
Guajataca Beach	0.0014
Jobos east	0.0015
El Maní	0.0011
Manatí –Arecibo Road #681 Station 2	0.0007
Manatí River Mouth	0.0004
Manatí –Arecibo Road #681 Station 1	0.0004
Guanajibo River Mouth	0.0004

X-ray test showed different sources of carbonate material in the samples. These are magnesium calcite, aragonite, calcite and dolomite. In El Faro beach aragonite and calcite were the carbonate present in the sample. Skeletal algae such *Halimeda* had an internal structure composed of aragonite and correlated with grain counting observation that showed the carbonate material in El Faro Beach that came from skeletal source (hard body parts of marine plants and animals as described by Tucker and Wright, 1990). In modern environments like beaches, mollusk class is the one that contains calcium carbonate secreting specie. The geologically important classes are *bivalve* and *gastropods* among others. (Scoffin, 1987).

Carbonated material in Tamarindo west and Tamarindo east are limestone material from onsite outcrop eroded by the wave as described of the Quaternary (Morelock 1978). X-rays analyzes both beaches found magnesium calcite, aragonite and dolomite. Magnesium calcite is the mineral that compound the skeleton of *echinoids* (sea urchins), *ophouroids* (brittle star) and *holothurians* (sea cucumber) (Scoffin,1987). Dolomite is a mineral requires time to precipitate (Tuker and Wright, 1990), therefore confirming one of the component of these grains came from erosion of previous depositions. The aragonite in these beaches also contains pieces that may be from the *Scleractinia* order which Scoffin describes as stony coral with hard aragonite skeleton, examples are *acropora* and *montastrea*.

The main difference in magnitudes of the reflectance curves of Tamarindo beaches can be related to the grain size distribution. As shown in Figure 11, Tamarindo west had poorly sorted grain size distribution, from medium to fine sand. Tamarindo east had a well sorted grain size distribution of medium sand. Tamarindo west had a second grain increment of fine sand ($< 2 \phi$) in the sample. In the visible region the finer the material the reflectance magnitude increased (Vincent, 1997)

These four beaches presented the highest spectral slope (Table 5). El Combate beach had the steepest slope (0.0022), which could be related to the quartz content. El Faro Beach, Tamarindo West and East had the same slope values (0.0017).

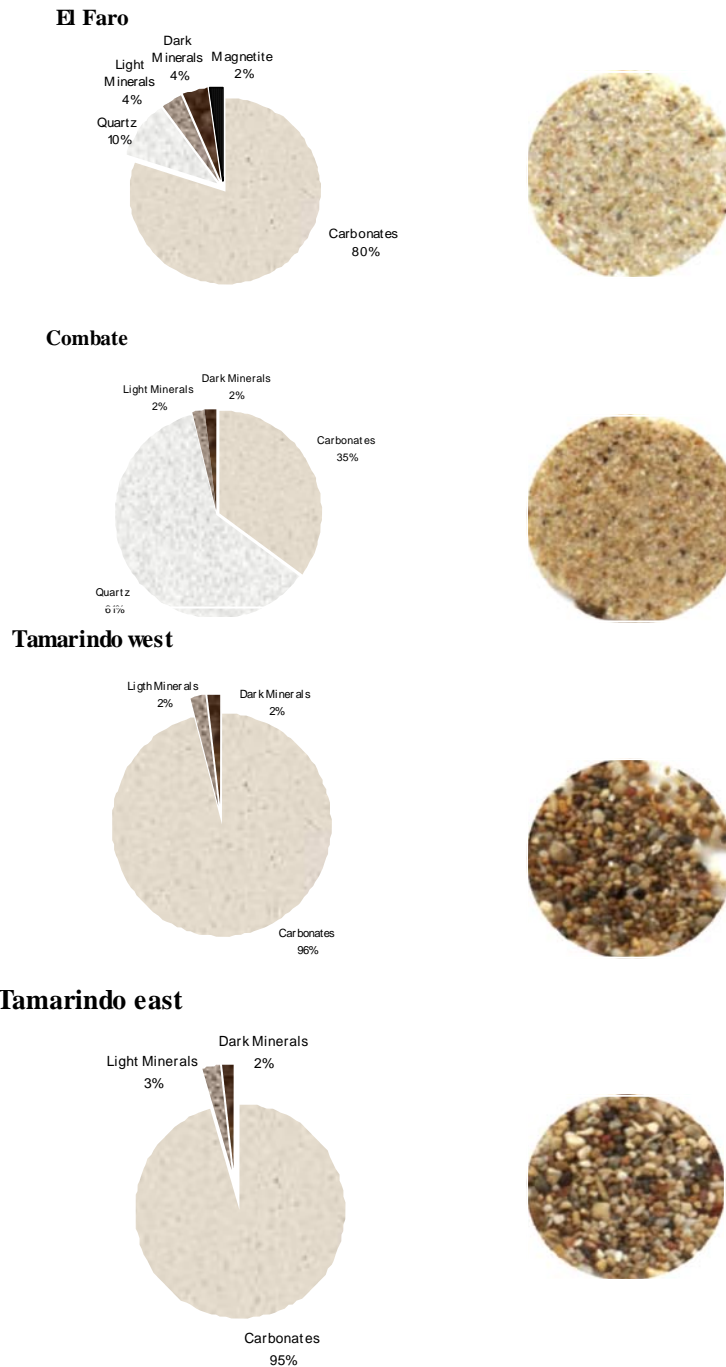


Figure 10: Grain count composition and picture of the sample for: a) El Faro Beach, b) El Combate Beach, c) Tamarindo West and d) Tamarindo East. The order follows the reflectance magnitude (from highest to lower).

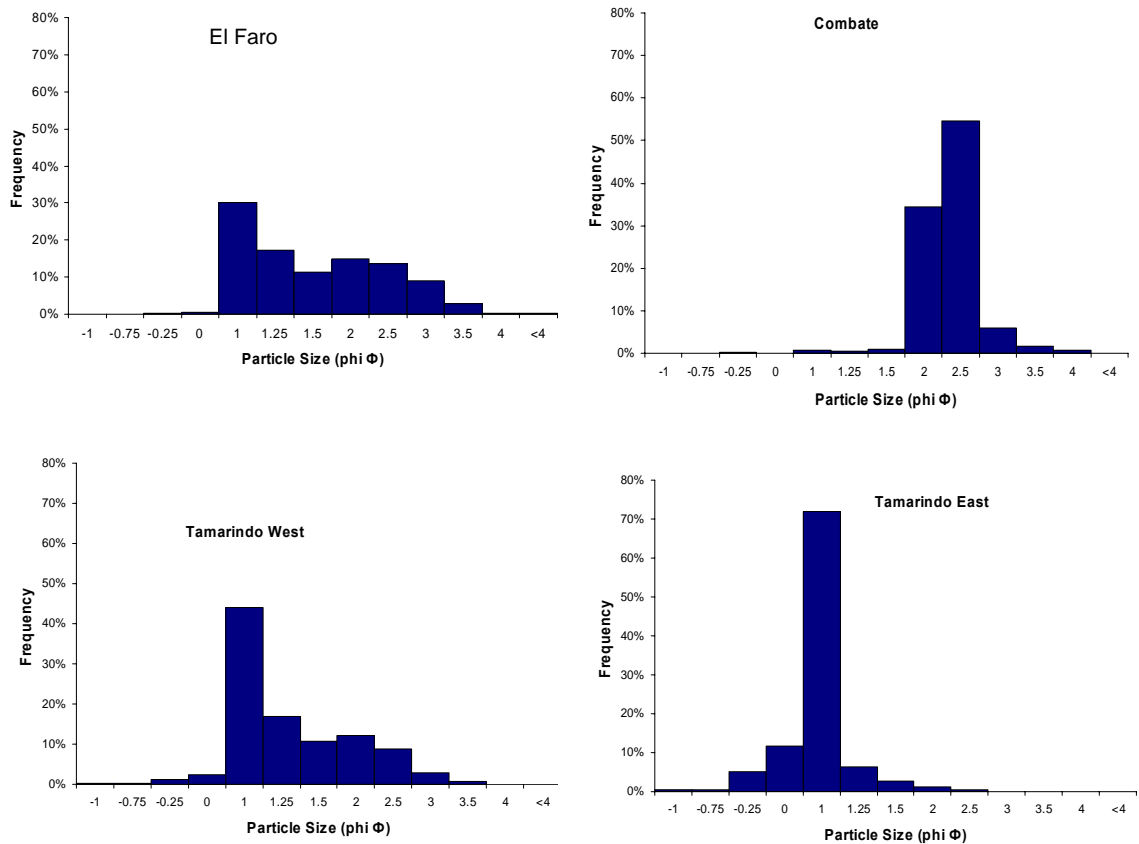


Figure 11: Grain size distribution for El Faro Beach, El Combate, Tamarindo West and Tamarindo East.

Crashboat, Jobos West, Station 3 of Manatí-Arecibo, and Córcega beaches had carbonate content from 47% to 55% (Figure 12). Inclusion of light minerals, dark minerals, and magnetite in these samples were responsible to lower the magnitude of the reflectance curve. X-ray analyses found albite, quartz minerals in these four beaches. The quartz found in the sample came from a variety of sources and fits under the light color classification, these grains tend to have other elements inclusions that make the grain change its color.

Crashboat had a 55% of carbonate content. Grain counting observations showed that the carbonate source from Crashboat (X-rays found magnesium calcite in the sand) is more light in color when it is compared with Córcega (X-rays found m calcite in the sand) that has the same carbonate percent.. These two beaches were similar in the mineral

distribution; 16% quartz, 12% light minerals, 11% dark mineral, and 6% of magnetite. They both showed very similar grain size distribution, from medium to very fine sand (1Φ to 4Φ). The 10% difference in their reflectance measurements is related to the source of these carbonate material. Personal observations of the magnesium calcite grains e.g. *echinoids* compare to calcite grains e.g. *bivalves*, magnesium calcite will be more light in color because in internally produce. Mollusk excretes the calcite that may have intrusions of particles altering the color of the surface.

Jobos west had a 49% of carbonate material, 28% of light minerals and 10% of dark minerals. Station 3 of Manatí-Arecibo had 47% of carbonated material, 27% of light minerals and 17% of dark minerals.

Jobos west showed a grain size distribution from medium to very fine sand (1Φ to 4Φ) with a peak concentration at 2Φ (Figure 13). In Station 3 from Manatí- Arecibo the grain size distribution ranged from very coarse sand to fine sand (-0.25Φ to 3Φ) with a peak concentration at 1Φ . The additional 7% of dark mineral and the 1Φ difference in grain size in Station 3 reduced the magnitude of the reflectance curve by 5% compare to Jobos West.

The slope of these beaches ranged from 0.0019 to 0.0016 suggesting that the slope is higher when the combination of carbonated and quartz material is more than 60% of the sample.

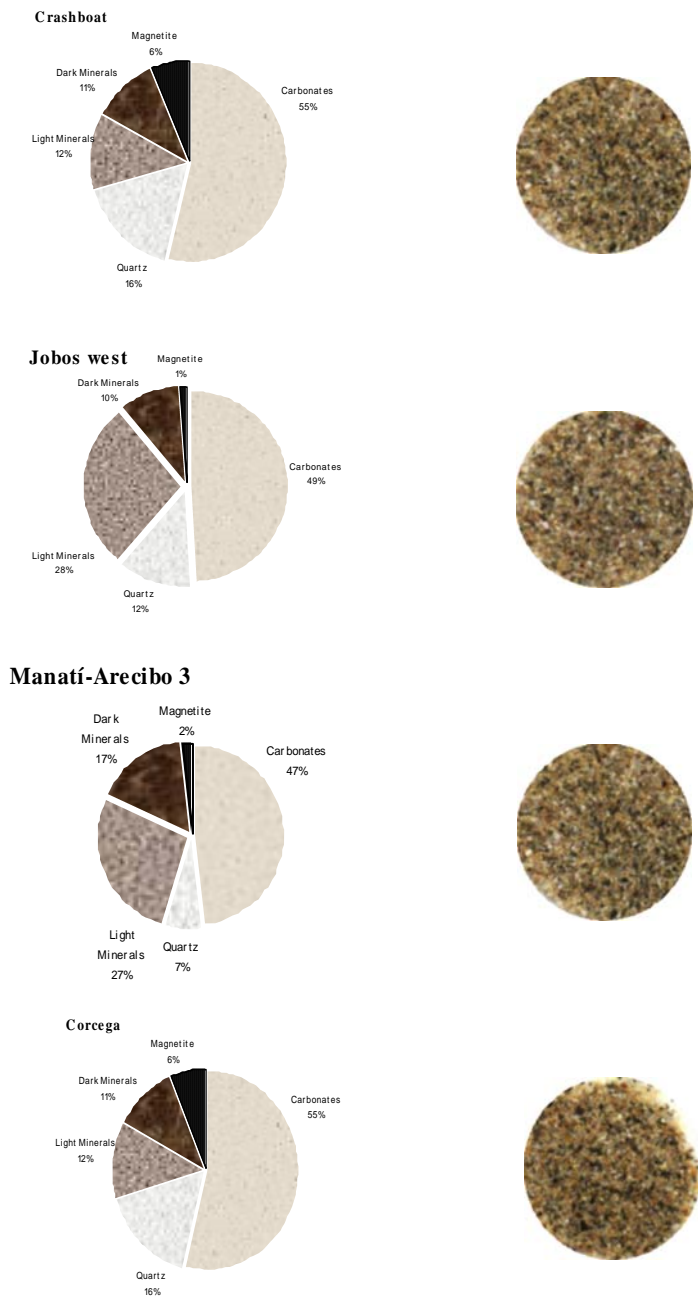


Figure 12: Grain counting composition for: a) Crashboat, b) Jobs west, c) Sta.3 Manatí- Arecibo and d) Córcega. The order follows the reflectance magnitude (from highest to lower).

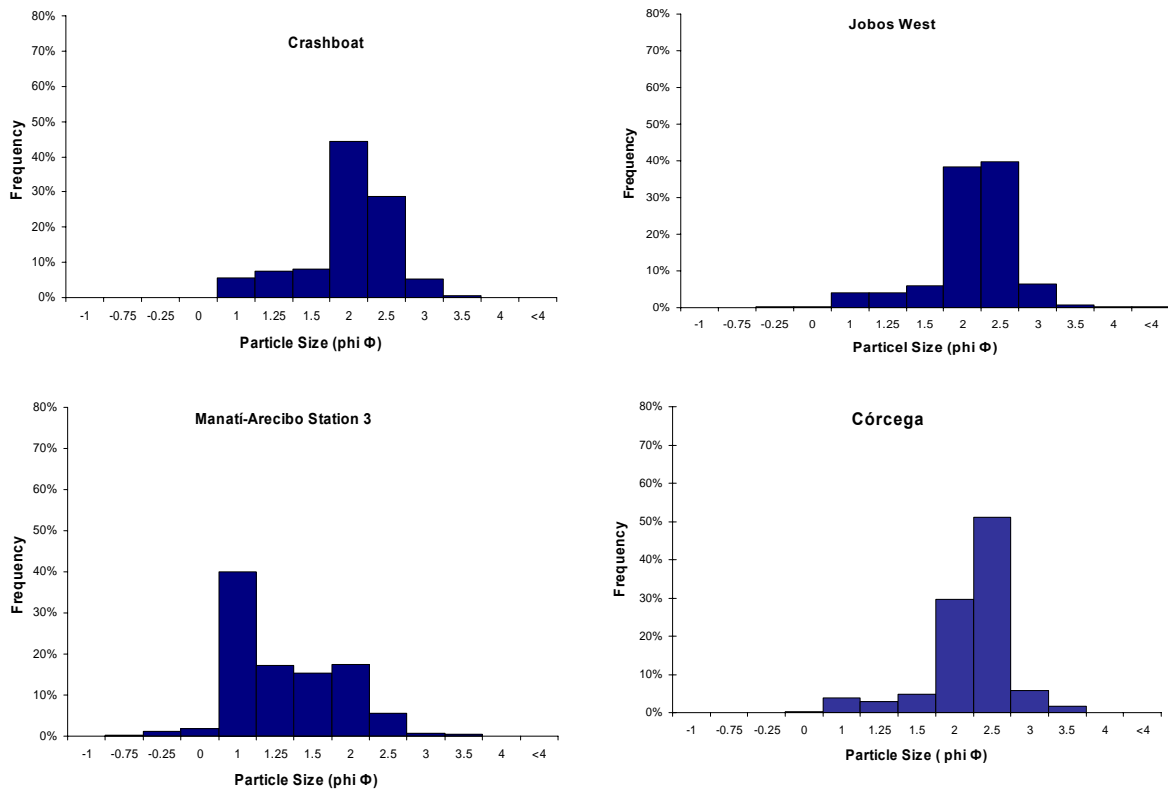


Figure 13: Grain size distribution for Crashboat, Jobos west, Station 3 from Manatí-Arecibo and Córcega

Guajataca, Jobos East, El Maní, and Station 2 of Manatí-Arecibo beaches were characterized by the increase of light minerals and dark mineral concentrations (Figure 14). Guajataca had 36% of light minerals, 15% of dark mineral and 8% of magnetite. Jobos East had 59% of light minerals and 13% of dark mineral. El Maní had 43% of light minerals and 33% of dark mineral. Station 2 of Manatí-Arecibo had the highest concentration of dark mineral with 40%. High light minerals and dark minerals reduced the magnitude of reflectance curves in these beaches. Xray measurements detect the presences of quartz (the non-colorless variety), albite and augite minerals.

However, the grain size distribution of these four beaches did not affect the reflectance curve as expected (Figure 15) it only follows the composition pattern instead of being affected by grain size. In Guajataca beach the grain size distribution ranged from coarse sand to very fine sand (-0.25Φ to 4 Φ). In Jobos East the grain size distribution ranged from granulated sand to coarse sand (-1 Φ to 1.25 Φ) the coarser sample of all beaches. In El Maní and Station 2 of Manatí-Arecibo the grain sand distribution ranged

between medium sand and very fine sand ($1\Phi - 4\Phi$), the increase in the dark minerals sources overlap the grain size. The slopes in these four beaches ranged from 0.0015 to 0.007, which was related with high light minerals and dark minerals concentrations in the samples.

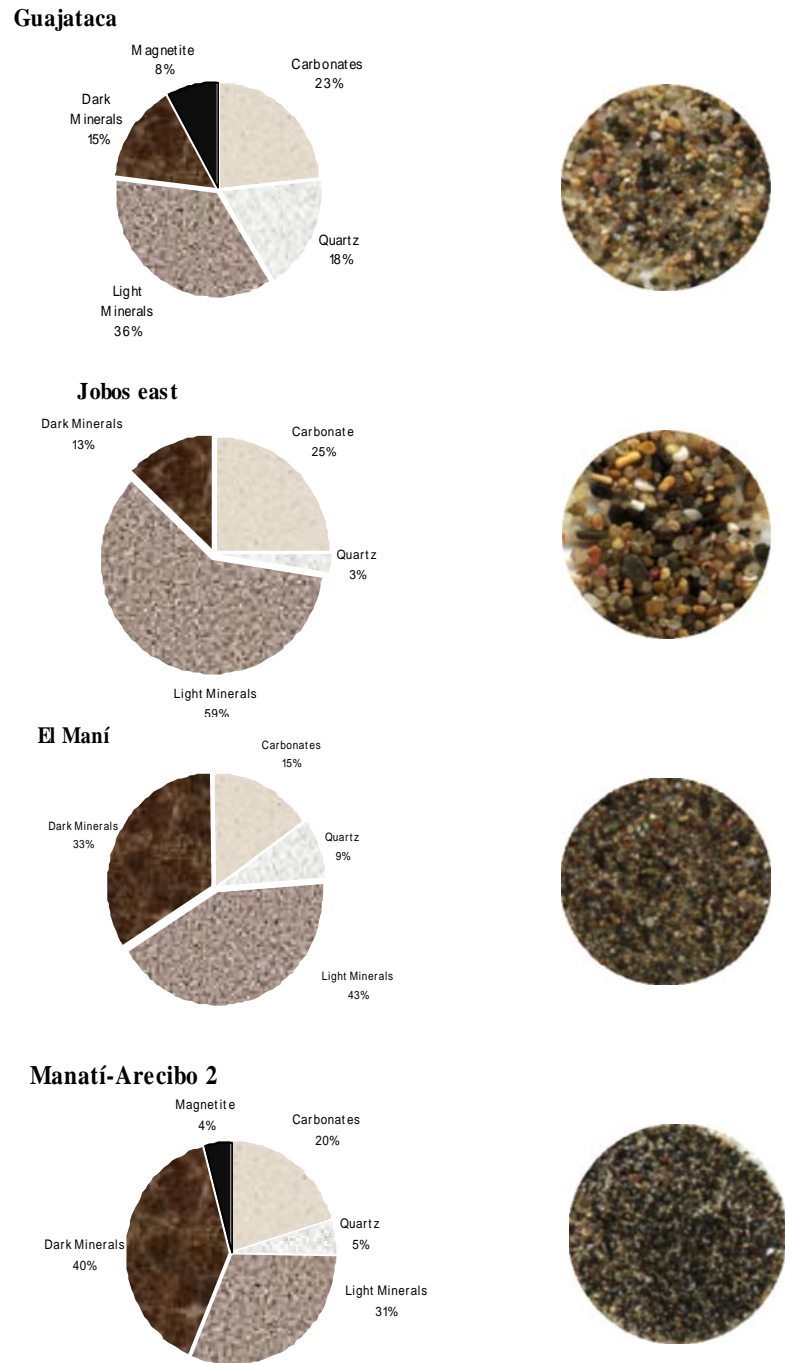


Figure 14: Grain counting composition for: a) Guajataca, b) Jobos East, c) El Maní and d) Station #2 Manatí-Arecibo. The order follows the reflectance magnitude (from highest to lower).

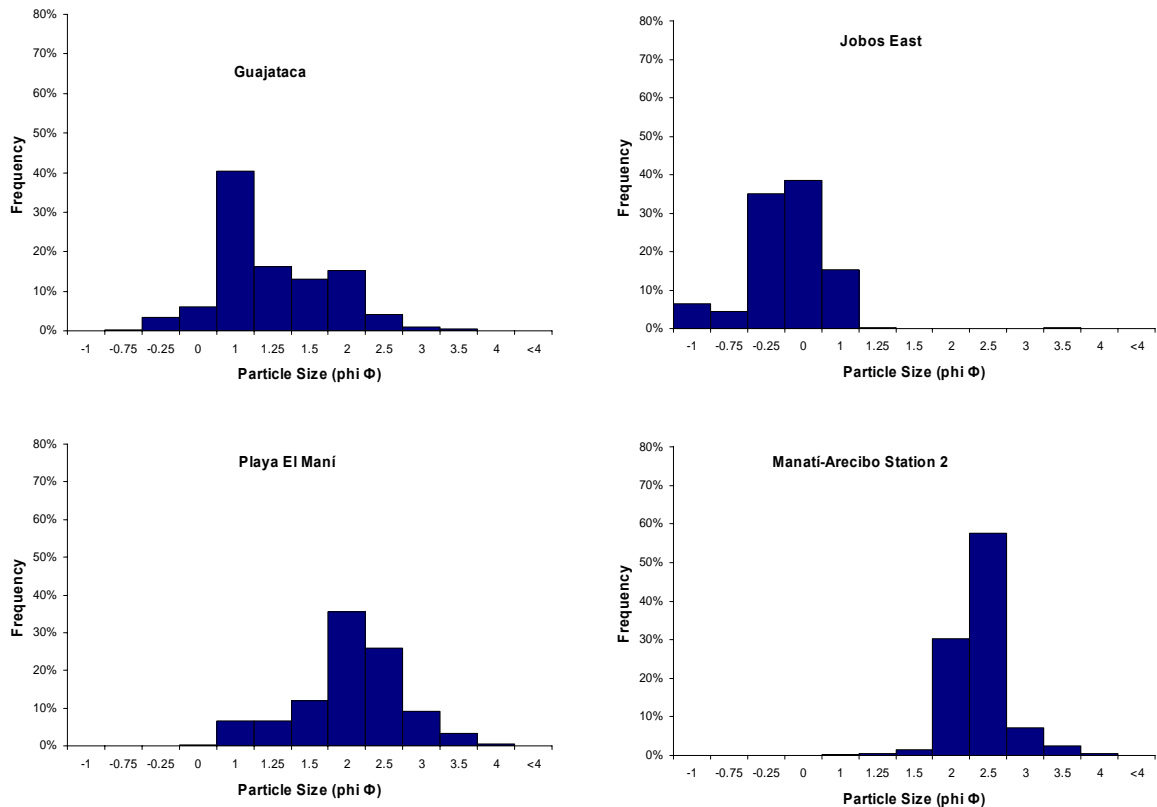


Figure 15: Grain size distributions for Guajataca, Jobos East, El Maní beach and Manatí-Arecibo Station 2

The last group of beaches in this study had the higher concentration of dark minerals (Figure 16). Manatí River mouth had a 60% of dark mineral and 21% of light minerals. Station 1 from Manatí-Arecibo had 40% of dark minerals and 36% of light minerals. X-rays analysis from Manatí River mouth and Manatí-Arecibo found quartz (non-colorless), augite, albite andradite and magnetite.

Guanajibo River mouth had the highest concentration of dark minerals with 67%, the light minerals was 31%, and only 1% of carbonated material Manatí River mouth had a higher concentration of dark mineral. X-ray founds albite, augite, and quartz (non-colorless) mineral grains.

The reflectance curve in this beach was 2% higher than Station 1 of Manatí-Arecibo beach. Observations in the grain counting showed bigger light minerals grains compare to the rest of the material in this sample. The size difference of the grain was of 0.5Φ observed in the laboratory analysis.

Grain size distribution for these three beaches ranged from coarse sand to fine sand as shown in Figure 17. These three beaches had the lowest spectral slope values (0.0004), and it was related to the high content of dark mineral in the sands.

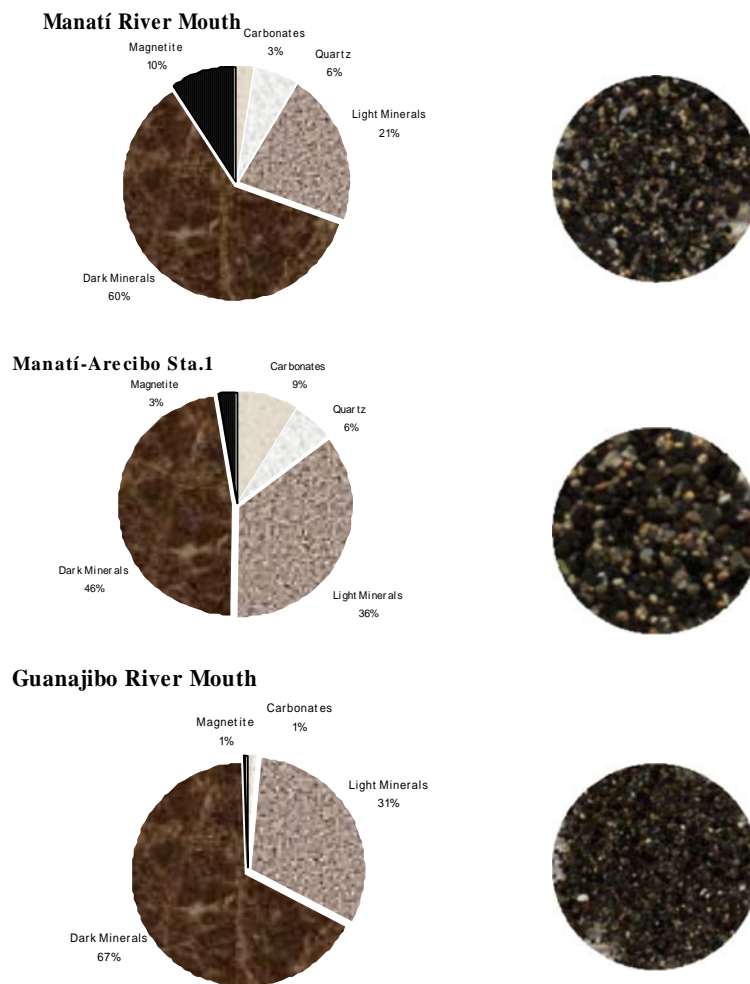


Figure 16: Grain counting composition for: a) Manatí River Mouth, b) Station #1 from Manatí-Arecibo, c) Guanajibo River Mouth. The order follows the reflectance magnitude (from highest to lower).

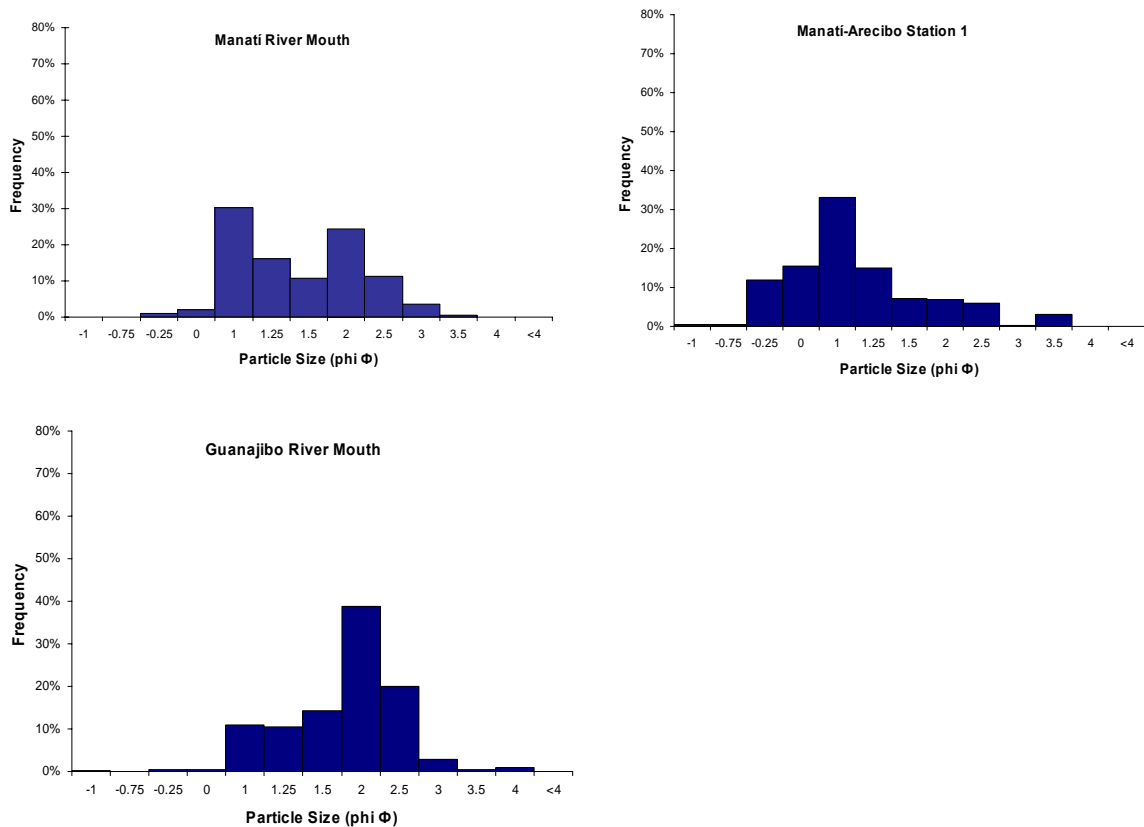


Figure 17: Grain Size Distribution Chart for Manatí River Mouth, Station #1 from Manatí- Arecibo and Guanajibo River Mouth

4.3 Laboratory Experiments

The samples used for these experiments were divided in three main categories based in the mineral composition; they were (a) Carbonates, (b) Dark Mineral, and (c) Quartz.

Two sets of samples were prepared using different sources of carbonate. Carbonates from El Faro Beach (Table 3) and Playa Tamarindo (Table 4) were combined to evaluate the changes in the reflectance curve and its spectral slope based on the composition of the sands. Sand from El Faro beach are high in aragonite and sand in Tamarindo beaches has more variety in carbonate sources; aragonite, magnesium calcite and dolomite.

4.3.1 Carbonate Comparison

Figure 18 shows the reflectance curves generated by the first set of samples with carbonate material from El Faro Beach which is mostly aragonite. Sample PM-1 with 100% carbonate material and grain size of 2Φ showed the highest reflectance. The sample called El Faro Beach followed in magnitude with a grain size of 1.5Φ which grain are coarse than 2Φ . The results demonstrate that finer material has more reflectance.

The magnitude of the reflectance curve decreased when the carbonate content in the sample also decreased from 100% to 70%. However, when light minerals were added in more than 10% this pattern is affected as shown in samples PM-4 to PM-7. These samples also contained quartz and magnetite, but there was not correlation with these minerals affecting the reflectance curve as much as the difference of carbonated percentage in the content. Magnetite represents less than 10% of the sample in any of the beaches studied and it is usually very fine grain ($<3\Phi$) in beaches of Puerto Rico.

Samples using carbonate material (magnesium calcite and aragonite) from Playa Tamarindo showed the same reflectance pattern as in El Faro Beach (Figure 19), but the magnitude of the curve decreased.

In Figure 19 the sample called T-round is 100% carbonate sand, in which all grain are polish and rounded. The source of this carbonate is Playa Tamarindo the grain size is coarse (1Φ). Its magnitude is lower than the sample TM-1 which is also 100% carbonate of Playa Tamarindo but finer grain size. Which confirm with the observations of both beaches, Tamarindo east and west, the main difference between these two is the grain size. (The sand of this beach for experiment purpose is 2Φ)

Figure 20 shows a comparison of the results from El Faro Beach and Tamarindo. They had the same pattern in reflectance, but the difference in magnitude in the reflectance curve is related to the carbonate source in the sample.

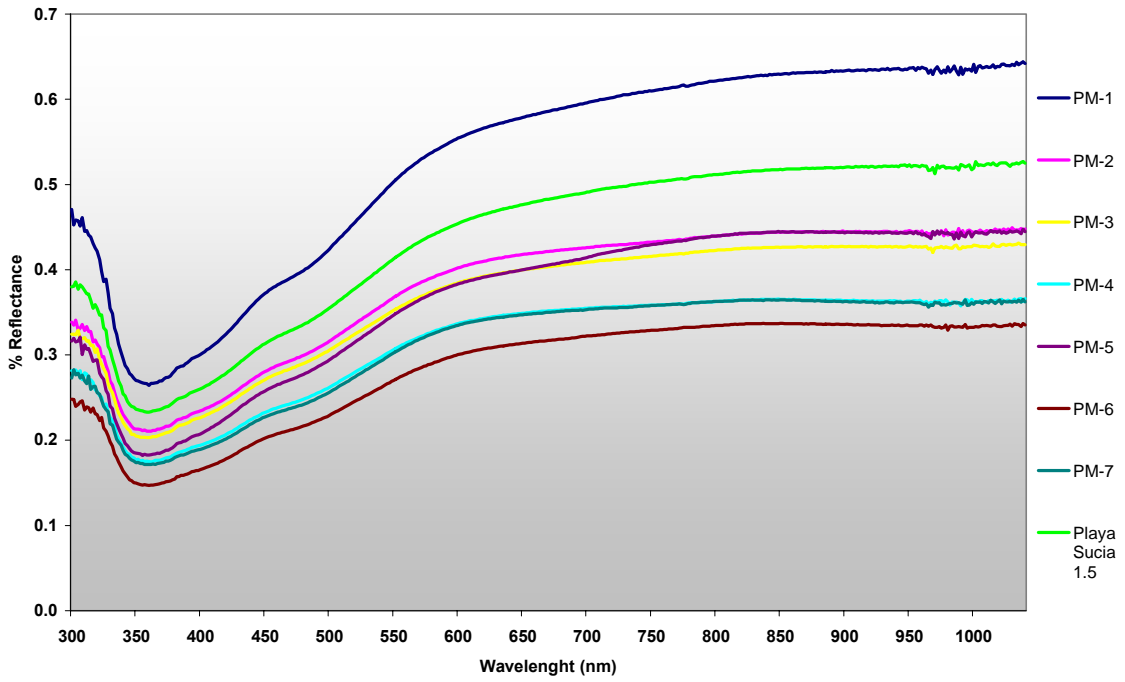


Figure 18: Carbonate material in these samples is from El Faro Beach. The graph show sample in which carbonate content is more than 40%.

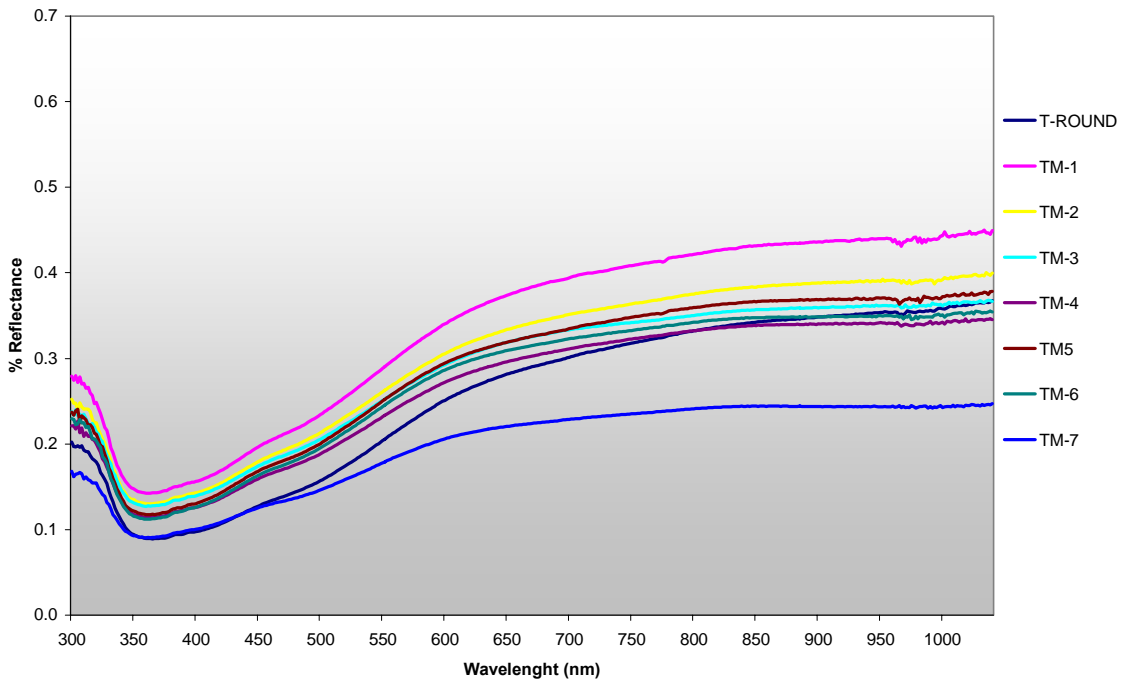


Figure 19: Carbonate material in these samples is from Playa Tamarindo. The graph show samples in which carbonate content is more than 40%.

Values of the spectral slope in the carbonate experiments ranged from 0.0010 to 0.0023. Samples with more than 40% of carbonate minerals had slopes among 0.0013 to 0.0016. These values increased when quartz is present in the sample, except for PM-1 that had a slope of 0.0023 with 100% carbonate sand grains of 2.0 Φ . Playa Sucia sample is also 100% carbonate material but with a grain size of 1.5 Φ and had a slope of 0.0017. Also sample T- round which are 1.5 Φ size sand from Tamarindo beach and has a slope of 0.0014 compare to TM-1 that in the same sand but finer material 2.0 Φ . The calculations suggest that the spectral slope is affected by grain size., but It seems that the difference of the carbonate material sources, aragonite, magnesium calcite or dolomite, does not influence the spectral slope of the sample.

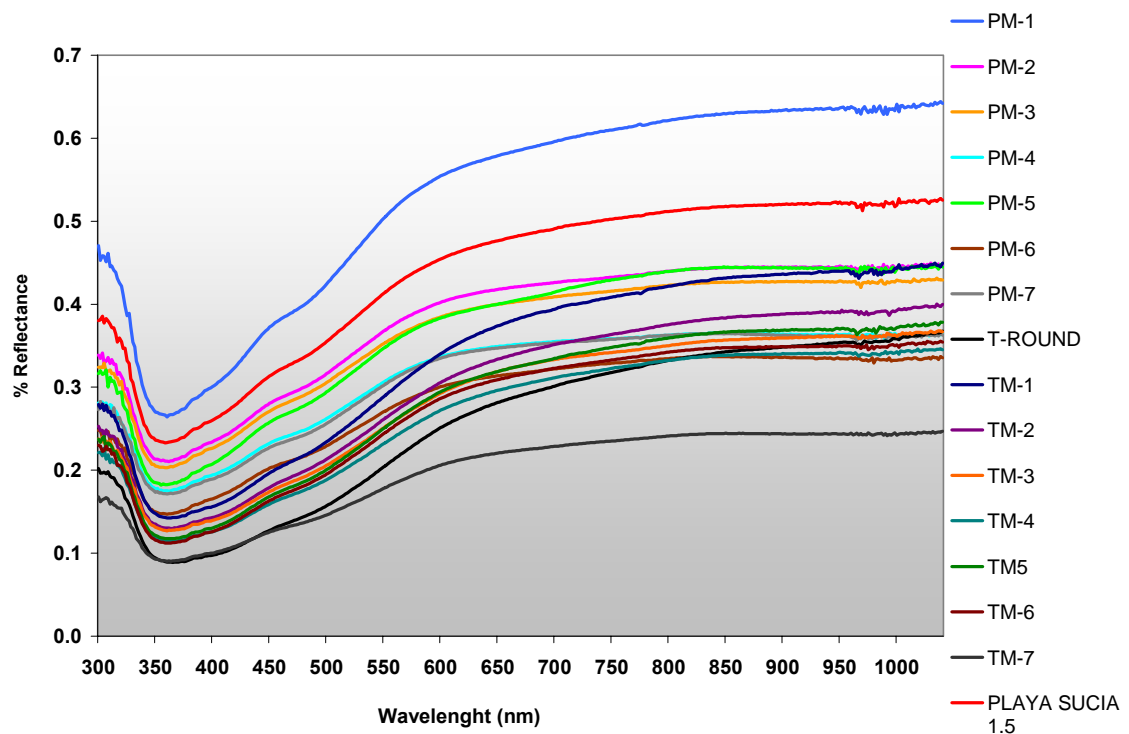


Figure 20: Carbonate Comparison with the two sources of carbonated material

4.3.2 Quartz Comparison

The higher colorless quartz content found in the analyzed samples was 60%, and it was found in western Puerto Rico (El Combate beach, figure 10). The magnitude of the reflectance curves was affected by low carbonate, high light minerals and dark mineral content (Figure 21). The sample identifies as Quartz corresponded to 100% of quartz content. Its magnitude was lower than the other curves in the 384 nm and higher in 706 nm. Tamarindo carbonate grain sand samples followed the same pattern as El Faro Beach in these quartz experiments (Figure 22) there were small differences in the magnitude between them (Figure 23).

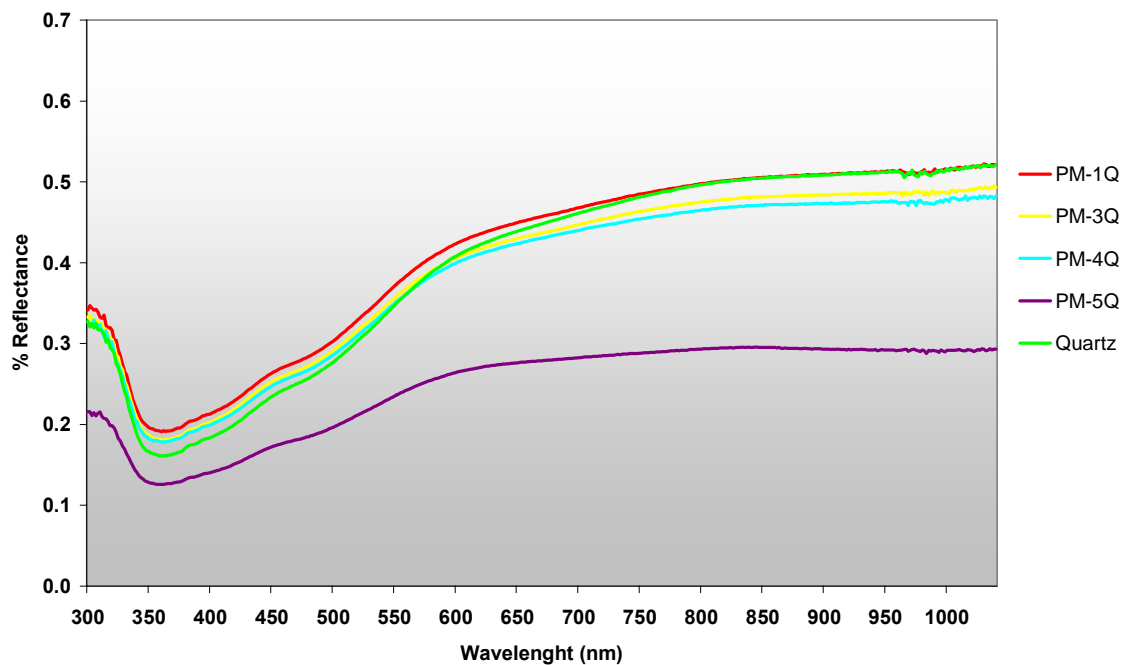


Figure 21: El Faro Beach carbonates source quartz comparison

The highest spectral slopes in the reflectance curves were produced with high quartz according to these experiments. Samples with more than 40% of quartz showed a spectral slope of 0.0018 or higher. This work suggests that colorless quartz grains in the sample affects more the reflectance curve than other materials. Observation of the graph suggesting that quartz reflects less in the blue range of the spectrum and more in the red range, creating steep slope between these two areas of the spectrum.

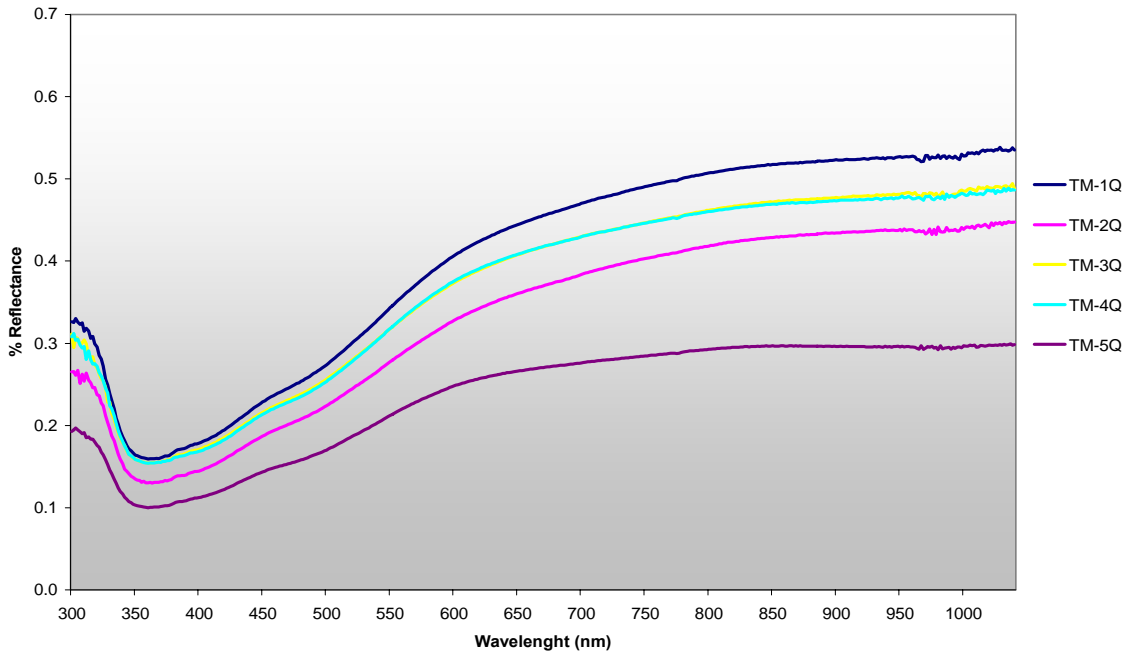


Figure 22: Tamarindo carbonate source quartz comparison

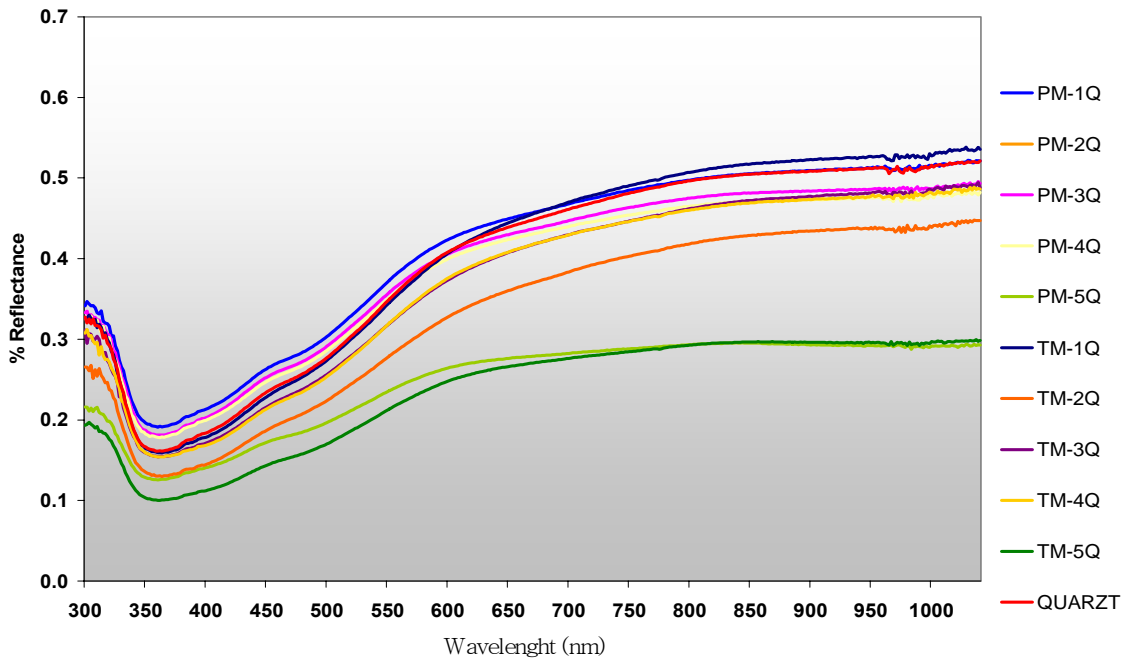


Figure 23: Quartz comparisons between the El Faro beach carbonate material source and Tamarindo beach source.

4.3.3 Dark Mineral Comparison

The dark mineral experiments considered samples with a maximum of 60% of dark mineral content and 50% of light minerals. These concentrations were used because usually in Puerto Rico dark mineral in beaches tend to have high light minerals mineral concentration. According to the experiments, considering different carbonate sources, low reflectance was related to high dark mineral content (Figures 24 and 25). Carbonate and magnetite concentration on these samples was fixed to 10%, base in the samples collected of the 15 beaches where high concentration of dark mineral beaches has low concentration of carbonate material.

Light minerals content ranged between 30% to 50%, but a direct relationship between these mineral concentrations in the sample and the magnitude of the reflectance curve was not found. In these experiments there was evidence that the sources of the carbonate material can affect the magnitude of the reflectance curve as shown in Figure 26, where Tamarindo sand sample values were lower than El Faro Beach sand sample

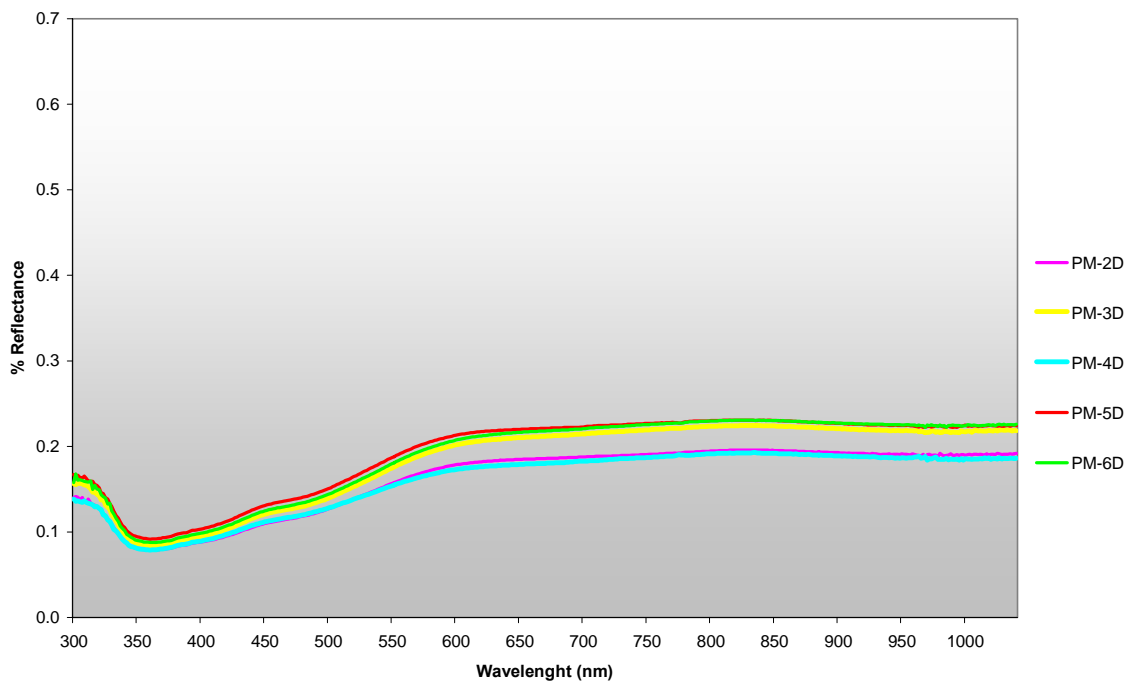


Figure 24: El Faro Beach carbonate source for dark mineral model.

values. Also, dark minerals in the sample reduced the value of the spectral slope, 30% or more of dark mineral generated a slope of 0.0013 or less, based on these experiments.

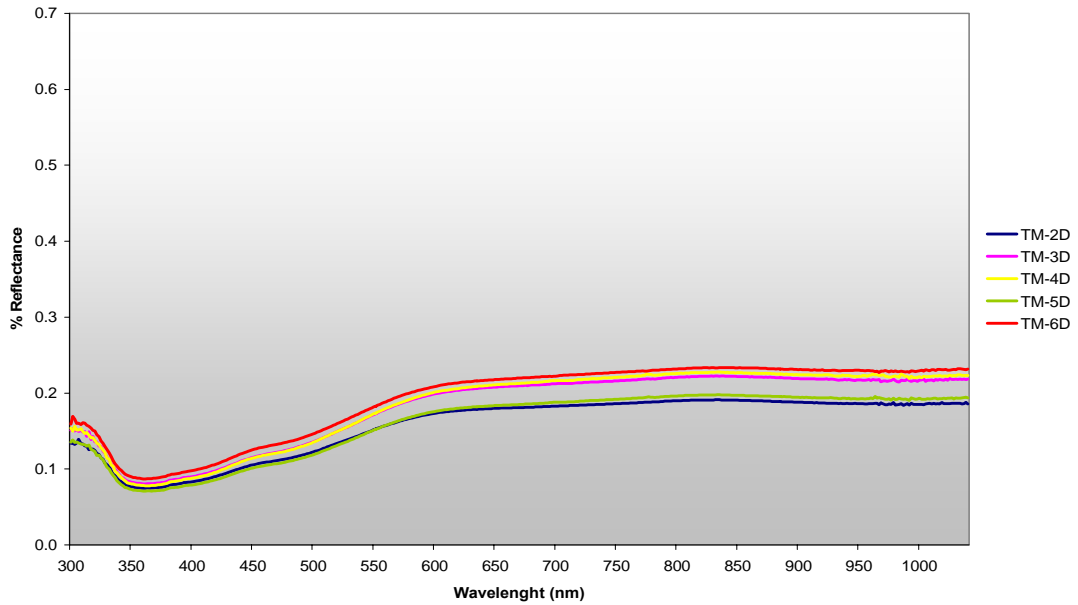


Figure 25: Tamarindo beach carbonate source for dark mineral model

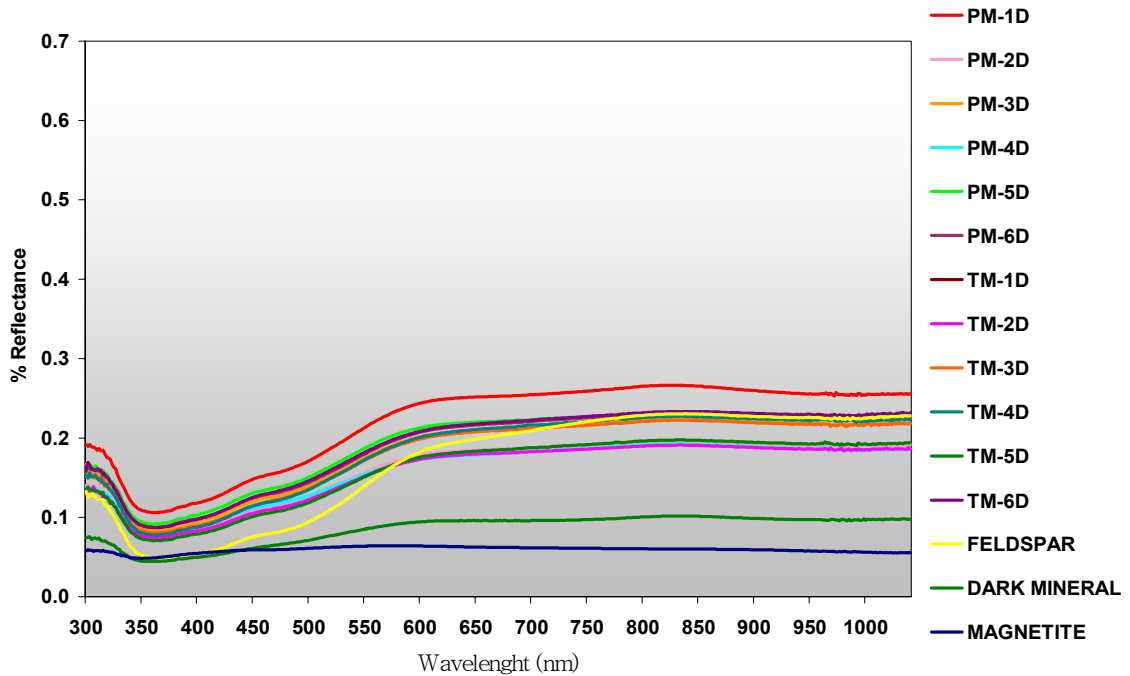


Figure 26: Dark Mineral comparison between El Faro Beach and Tamarindo carbonate source

4.4 Band Ratios Comparison

Band ratios for every beach calculated using data from the GER-1500 spectroradiometer and the IKONOS images (Figure 27) presented in Figures 28, 29, 30 and 31. A clear trend between the maximum and minimum values of the ratios was found in both datasets. This produced a good linear correlation between them. The main difference was found in the magnitude of the IKONOS data. Similar values were found for band ratios B1/B2 and B2/B1 when GER-1500 and IKONOS data are compared. Band 1 and Band 2 are the blue and green respectively. These two bands are located where the slope of the reflectance curve shows the major changes (Figure 9). Band ratios B3/B4 and B4/B3 also correlated well, except for El Faro Beach and beaches with 33% or more of dark minerals. Band 3 is red and Band 4 is Near Infrared.

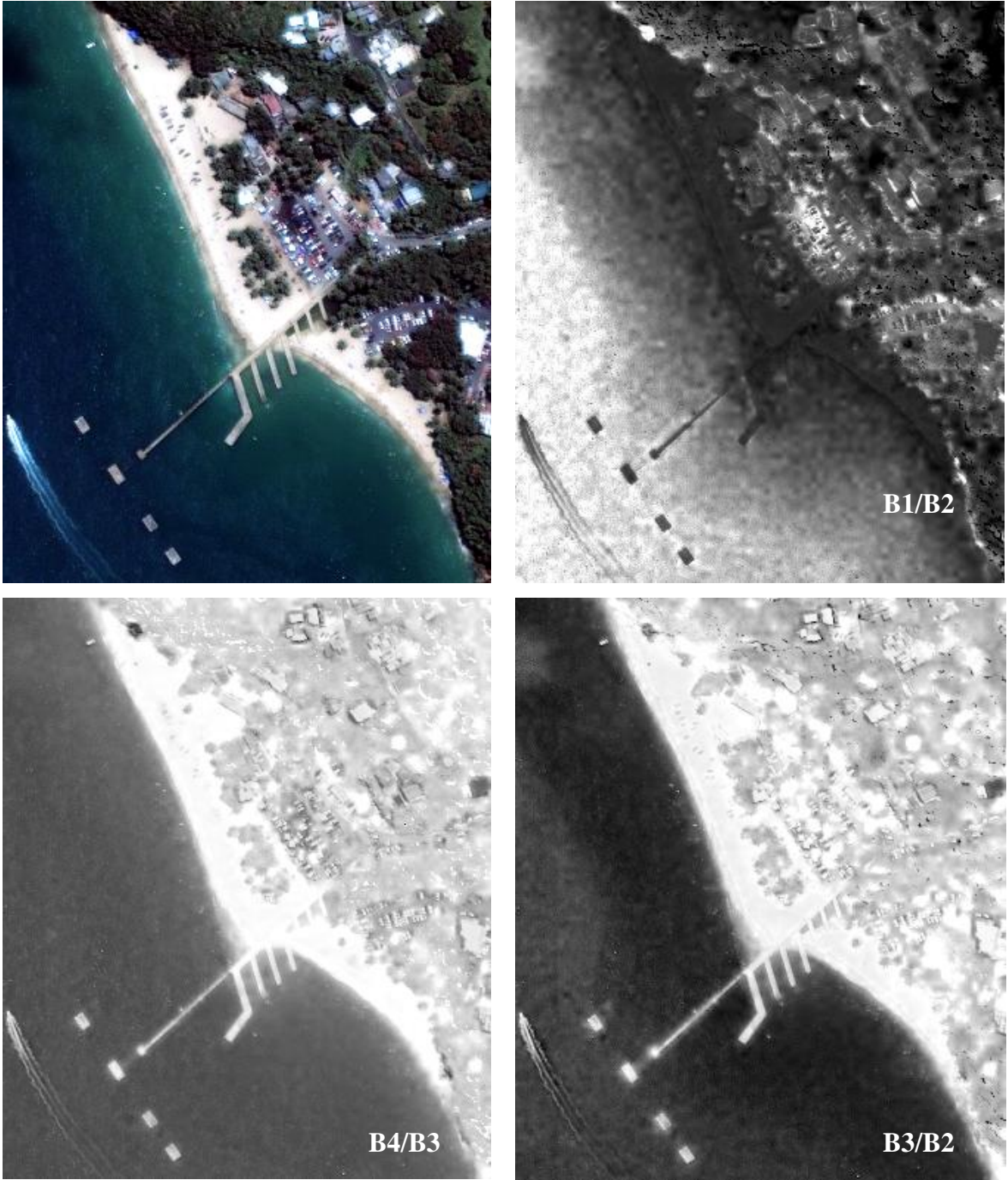
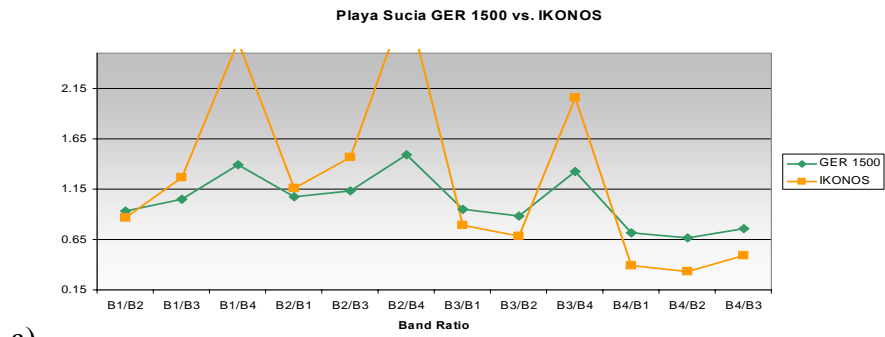
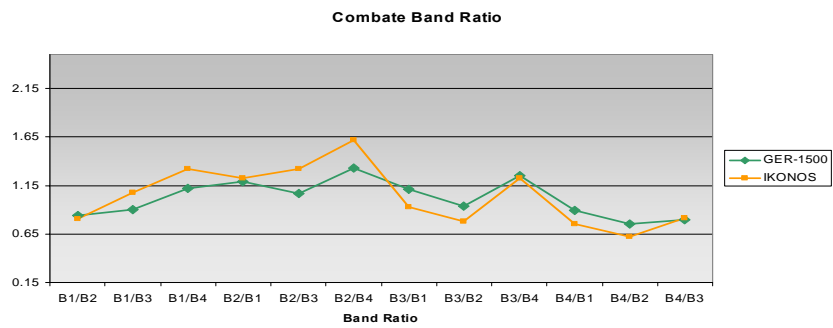


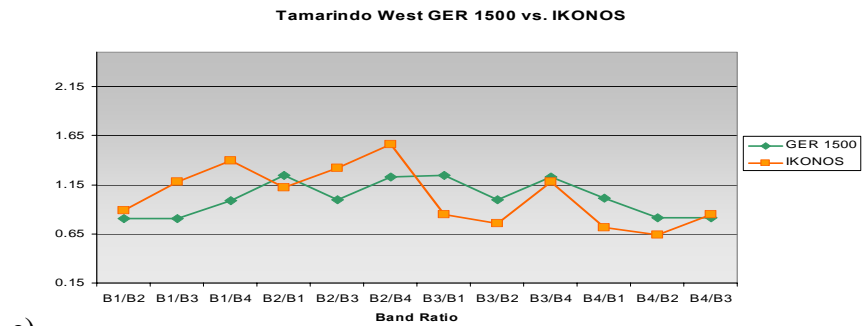
Figure 27: Example of IKONOS band math. The beach is Crashboat, Aguadilla. Band ratios B1/B2, B4/B3 correlates with GER data. Last image is B3/B2.



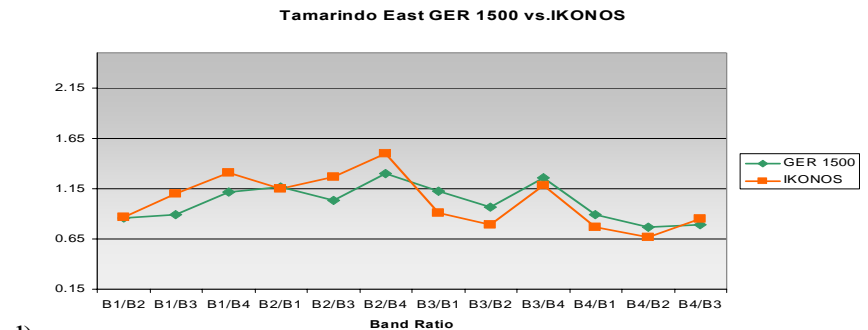
a)



b)

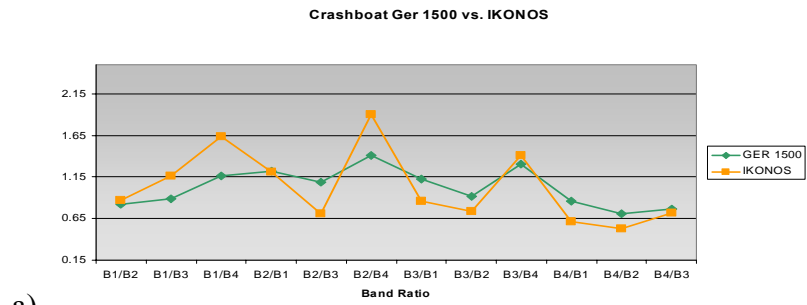


c)

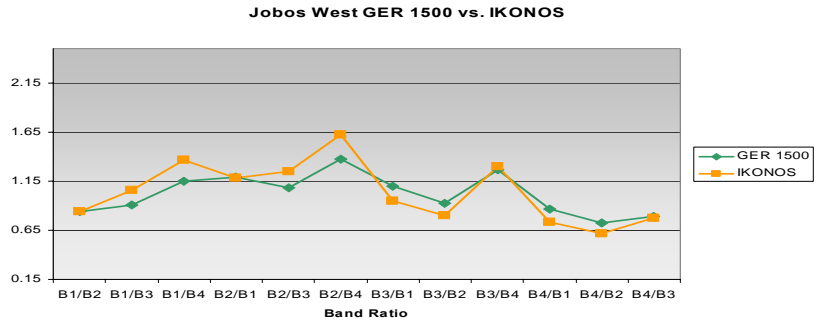


d)

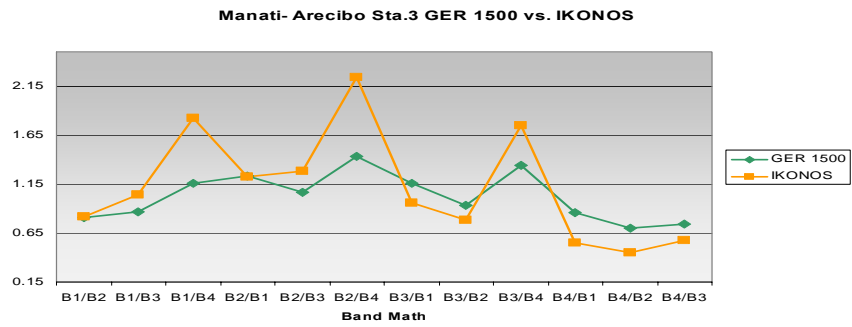
Figure 28: Band Ratio comparison between GER 1500 and IKONOS for a) El Faro Beach, b) El Combate, c) Tamarindo west and d) Tamarindo east 43



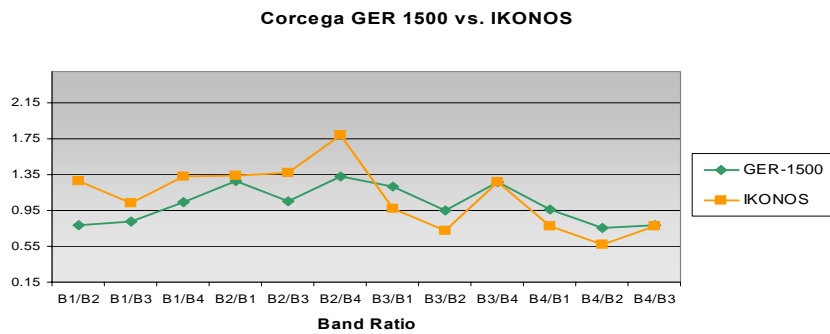
a)



b)

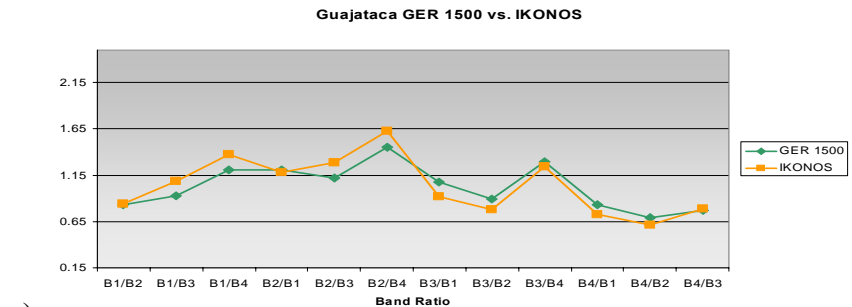


c)

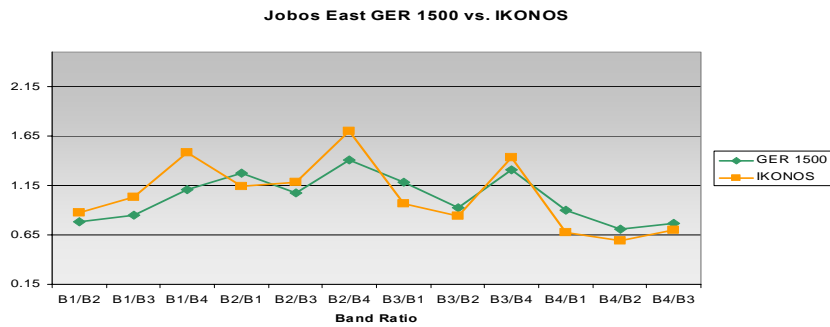


d)

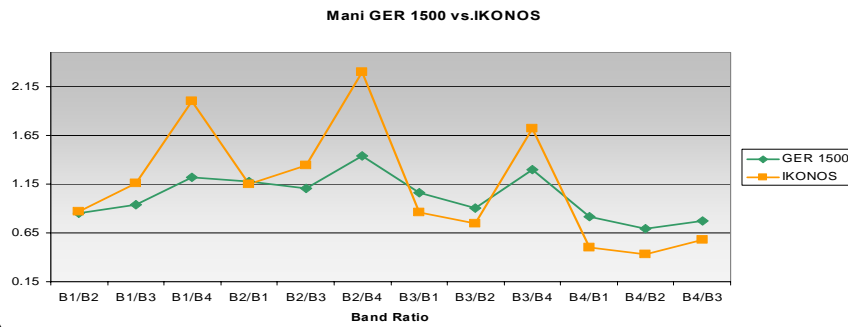
Figure 29: Band Ratio comparison between GER 1500 and IKONOS for a) Crashboat, b) Jobos West, c) Manatí-Arecibo 3 and d) Córcega



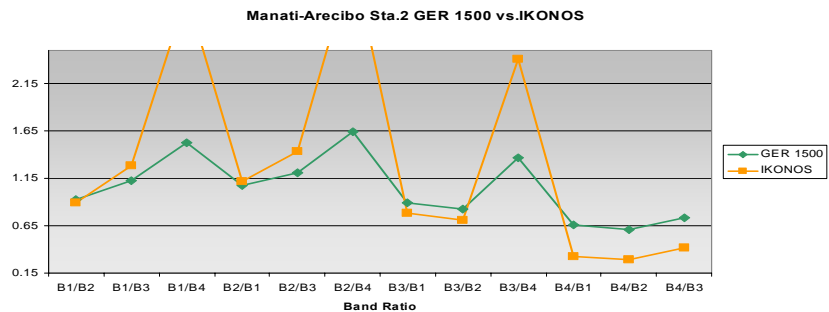
a)



b)



c)



d)

Figure 30: Band Ratio comparison between GER 1500 and IKONOS for a) Guajataca, b) Jobos East, c) El Maní and d) Manatí-Arecibo 2

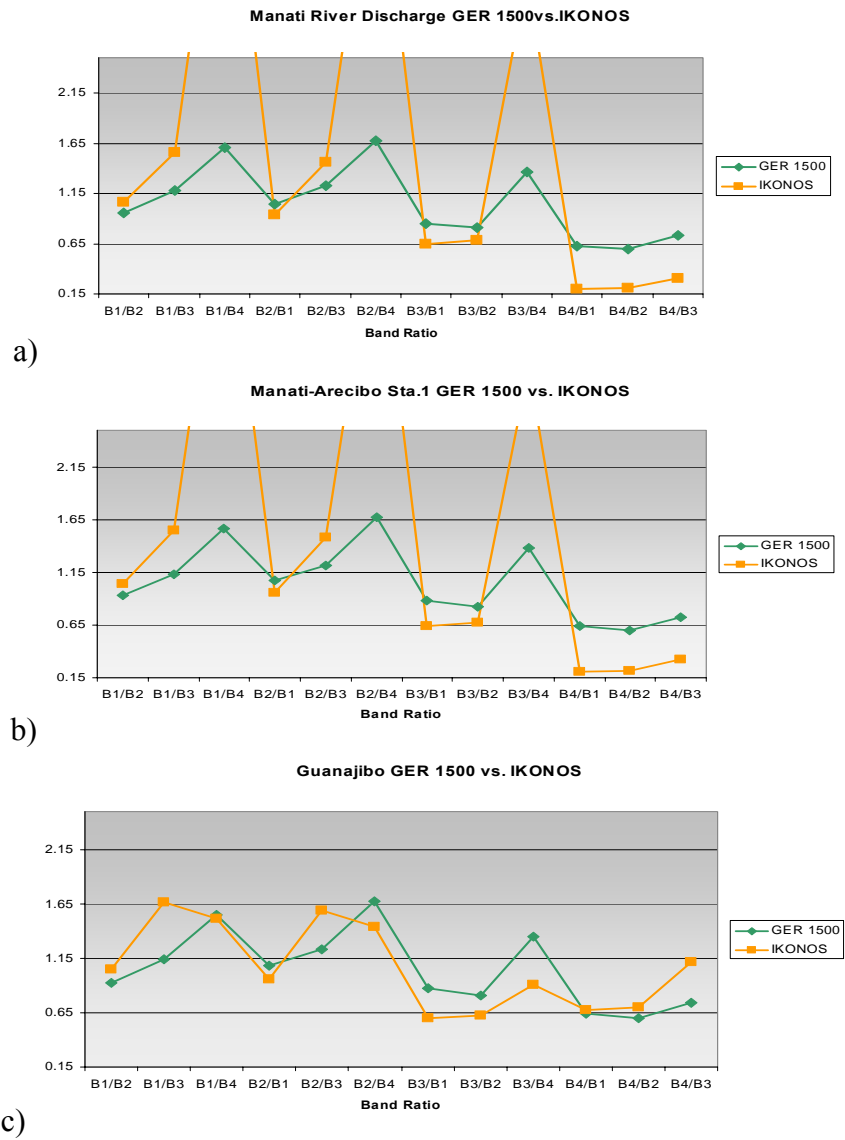


Figure 31: Band Ratio comparisons between GER 1500 and IKONOS for a) Manatí River Mouth, b) Manatí-Arecibo 1, and c) Guanajibo

4.5 Statistical Analyses

Statistical tests were performed to determine which band ratio of IKONOS data compared better with GER-1500 data.

A T-test for paired data showed that there was not significance difference between the ratios calculated with GER-1500 and IKONOS using B1/B2, B2/B1, B3/B4 and B4/B3 ($\alpha=0.01$; Table 5).

Table 6: T-test for paired results

Band Math	t	Results
B1/B2	1.906	Pass
B1/B3	8.661	Failed
B1/B4	3.119	Failed
B2/B1	1.602	Pass
B2/B3	4.538	Failed
B2/B4	3.378	Failed
B3/B1	12.474	Failed
B3/B2	14.477	Failed
B3/B4	2.212	Pass
B4/B1	7.168	Failed
B4/B2	5.692	Failed
B4/B3	1.757	Pass
$t_{0.01(2),14} =$	2.977	
n=15	v=14	

All other band ratios failed the test. Comparison of field and IKONOS data showed that the best band ratios to study sand are B2/B1 and B4/B3.

The relation between the B1/B2 or B2/B1 could be relate with the slope of the reflectance curve in this area of the spectrum (see figure 9), when is observe all beaches or all sand measurement in this research show a low reflectance value in the blue area of the spectrum and a high reflectance in the red and IR. This particular shape of the reflectance curve may be related to a specific signal from sand material.

Chapter 5

Discussion

Sand beaches have a unique spectral signature in the visible and near infrared. Reflectance curves for the 15 beaches show that the composition affects the magnitude of these curves. When mineral content in the sand begins to change with more igneous material, the magnitude of the curve gets lower. This was demonstrated in the experiments and in the field measurements.

The results found in this study show a correlation between the composition of the sand and the reflectance curve in the visible range of the spectrum. In the five categories where minerals were classified, carbonate material and dark mineral grains are the ones that affect the magnitude of the reflectance curve. Grain size also affects the magnitude of the reflectance curve and this was observed in some of the results obtained.

X-ray analysis shows that the carbonate materials available in the beach were aragonite, calcite, magnesium calcite and dolomite. Each one of these grains came from different sources. Aragonite grains are present in the beaches with the highest reflectance curve like El Faro beach and El Combate beach. This may be related to the fact that usually aragonite is formed inside of an organism like skeletal algae or like the case of corals that is surrounded by polyps (Scoffin, 1987), this grain looks white. In the case of the calcite or magnesium calcite like *mollusk* and pieces of *echinoid* torn, grains tend to be like beige in color, based on observation during the grain counting analysis. Therefore when these grains are in the sample they tend to lower the magnitude of the reflectance curve as observed in the sample obtained from the beach and from the experiment, when comparing the El Faro beach sand and the Tamarindo sand. Besides the difference between the carbonate grains, a clear pattern with the quantity of carbonate material in the sample shows that high concentration of these minerals increases the magnitude of the reflectance curve.

Light minerals do lower the reflectance curve magnitude when compared with carbonate material, but a pattern following concentration vs. magnitude was not observed. A variety of minerals classified under this category, X-ray analysis found the feldspar

grains albite as a common component of the beach even when feldspar is minerals unstable for beach environment. Another mineral that is abundant in this category is quartz in its non-colorless form. Quartz is one of the most abundant mineral in the planet and is highly resistant to weathering, it can be found in almost every color (Raymond, 1994) and then an important component of beach sand.

Quartz category includes the colorless form of this mineral, these grains are just colorless. They tend to be white in the samples that were analyzed. When these grains are with other grains like El Combate beach, when quartz and aragonite mineral are present it tend to have a high magnitude in the reflectance curve. But when is combine with other minerals as observed in the laboratory experiment, it tend to reflect the light characteristic of those others minerals, hence affecting the reflectance curve, decreasing its magnitude. Even when this quartz grains are mixed with other minerals, they have a lower reflectance in the blue range of the spectrum and high reflectance in the red and IR of the reflectance portion of the curve, having a high slope value (Table 3 and 4).

Dark minerals beaches have the lowest reflectance magnitude of all categories, these minerals reflect less light, according to the reflectance. When the darks minerals content is more than 40% in the sample, the curve tends to be flatter. The slope calculations are the lowest, less than 0.0012. These minerals tend to affect the behavior of the reflectance curve like the carbonate. In this case the higher the concentrations of the dark minerals in the sample the lower the reflectance curve magnitude.

Magnetite grains are present in most beaches in less than 10%, because this grain are small (3Φ or less) there are not significant when measure the composition of the sand. In the field and in the laboratory experiments magnetite content did not affects the behavior of the reflectance curve.

Beside the composition of the sand, the grain size is another factor to considered affecting the reflectance curve, as Vincent in 1997 state, in the visible area of the spectrum the finer material will have higher magnitude in the reflectance curve. This fact was observed in the field sampling in Tamarindo beach east and west, and in the experiment analysis with El Faro carbonate and Tamarindo carbonates. The difference

was of 5% in magnitude. Decreasing the grain size, increase the number of mirrors off which the light reflects (Vincent 1997) hence finer material will reflect more. However observations of the different experiments, when comparing the effect of the composition versus grain size over the reflectance curve, composition influence the reflectance more than grain size, but it is necessary to study this effect like it have been done with the composition in this research.

From the experiments it was possible to obtain composition of the sand using reflectance curves, in order to do this the spectral slope between B1 and B2 (blue and green area of the spectra) has to be calculated. The laboratory experiments shows that the slope value for carbonate sample is the same no matter the source of the carbonate material. The slope ranged between 0.0013 and 0.0016 with more of 40% of carbonated content in the sample and when the concentration any other material are less than 30%.

Sand mixtures with carbonate and quartz material (that represent more than 60% of the sample) will reduce the reflectance curve, probably because to the fact that in some cases quartz grains are colorless and will tend to reflect less. But slope values are higher (0.0016 -0.0019) than samples with more carbonated material.

In the laboratory experiments when colorless quartz is present with other grains, sand material such light minerals or dark mineral will lower the reflectance magnitude. The calculation of the slope will tell the presence of quartz in the sand. Quartz material produce high values (more than 0.0018) of the slope when is present in more than 40% in the sample.

When comparing the data obtained from the GER 1500 in the field with IKONOS images, band ratios correlate well, but the magnitude in the IKONOS data was higher. A possible explanation is the atmospheric effect. The main difference of the sand in the spectral behavior is in the magnitude and the band ratio provide little information about the difference between them (Campbell, 1997). However the relation between Band 1 and Band 2 for sand helps to predict sand composition when reflectance is compare.

Comparing the results with the previous work done by Morelock in 1978 only a few changes were observed in these beaches. In the Manatí river mouth beach dark

minerals dominate the sample. Morelock explains that there is a slow decrease of these minerals and an increase of carbonate material toward Arecibo (Figure 1). Samples Manatí-Arecibo Station 1, Station 2 and Station 3 agree with this statement. Manatí-Arecibo Station 1 has a 46% of dark minerals and 9% of carbonate material, Manatí-Arecibo Station 2 has 40% of dark minerals and 20% of carbonate material and Manatí-Arecibo Station 3 in Arecibo has 17% of dark material and 47% of carbonate material. Guajataca beach and Jobos east beach remain with same sand composition. Jobos east in the other hand shows a high concentration of light minerals material (59%) compare to the previous studies. This beach has coarser sand (0.25Φ) there is no river close for deposition, and grain is coarser for wind deposition or current transport. The light minerals came from erosion of the outcrop. Crashboat shows an increase in carbonate content when compared to 1978 which beach sediment was composed of equal amounts of carbonate, quartz, light minerals and dark minerals. The source of the carbonate is mostly skeletal fragment of echinoids (magnesium calcite). Córcega, el Maní, Guanajibo, El Combate, El Faro Beach and Tamarindo remains with the same composition.

Chapter 6

Conclusions

A general relationship between reflectance measurement and sand composition was established for the visible and near infrared range of the spectrum. It is possible to determine when one of the mineral categories are present in more than 40% of the sample (other mineral are present in concentration of 40% or less) and related this data to the remote sensing measurement, either obtained by a hand spectroradiometer or satellite image. Now there is a tool available to use them in sand sediment analysis.

The methodology to obtain composition of the sand using the reflectance curve based on the results of this study is calculated as following:

- If more than 40% of the sand comes from the sea by wave deposit, (carbonate sand from skeletal source, mostly aragonite and some magnesium calcite) reflectance curve will be higher than 30% in the magnitude and the spectral slope will range between 0.0013 and 0.0016.
- Beaches with carbonate content from erosion or weathering deposits (some calcite and dolomite minerals) in more than 40% of the sample, the magnitude of the reflectance curve will range between 20% - 30% and the slope will range between 0.0013 - 0.0016.
- Quartz in its colorless form in sand sample can be measured calculating the slope of the reflectance curve. When quartz is more than 40% in the sample, the slope will be higher than 0.0018.
- Dark Minerals can be measured when concentrations represent more than 40% of the sample. The magnitude of the reflectance curve will be less than 20% and the slope will be less than 0.0013.

Even when the visible and near infrared regions of the spectrum are not very precise to determine the exact composition of the sand, this study shows that it is possible to have a general idea of the composition by using high resolution sensor (1m) with low spectral range to monitoring drastically changes in sand composition.

However several key factors must be considered:

1. Carbonate source in beaches are crucial to explain the geology the area, aragonite fragment will have more reflectance than any other carbonate grains, these can be confused with light minerals, then again calculating the slope is possible to know the carbonate concentration in the sample.
2. Quartz grain with it colorless properties enhance the response of the other grains in the sample that affect the curve. Calculating the slope, quartz will tend to have the higher value.
3. Dark mineral in concentration of 30% or more will reduce the reflectance curve and the slope.
4. Trying to predict and specific composition of the sand using the visible range of the spectrum will not be accurate. In other hand, it is very helpful for a rapid analysis of beach sand or when analyzing images if compare with spectral libraries.

Further studies in sand beaches have to include the behavior of the curve with other types of carbonate material. If the material is available, quantify the effect of grain size.

The spectral library derived from this study is available through Dr. Fernando Gilbes Santaella, Geology Department of the University of Puerto Rico at Mayagüez.

Chapter 7

Literature Review

- Barreto, M., 1997, Shoreline Changes in Puerto Rico (1936-1987): Mayagüez Campus, University of Puerto Rico, unpublished Ph.D. thesis, 278p.
- Bawiec, W. J. 2001, Geology, Geochemistry, Geophysics, Mineral Occurrences and Mineral Resource Assessment for the Commonwealth of Puerto Rico, US. Geological Survey Open File report 98-38
- Cameron, A. 2003, Spectral Characterization of sand sediment west Puerto Rico: Mayagüez Campus, University of Puerto Rico, Department of Geology, Unpublished undergraduate paper, 14p
- Cambell, J.B. 2002 Introduction to Remote Sensing: New York, The Guilford Press, 621 p.
- Cracknell A P, 1999. Remote sensing techniques in estuaries and coastal zones an update. International Journal of Remote Sensing, 19(3), 485-496
- Crowley, J.K., 1986. Visible and near infrared spectra of carbonate rocks: reflectance variations related to petrographic texture and impurities: Journal of Geophysical Research, 91: 5001-5-12
- Deronde, B. 2004 Sand dynamics along the Belgian Coast based on Airborne Hyperspectral data and Lidar data. EARSel eProceedings 3, 26-32
- Folk, R. L. 1980, Petrology of Sedimentary Rock, Hemphill Publishing Company, Austin, Texas. 190p.
- Hunt, G. R., 1977, Spectral signatures of particulate minerals in the visible and near infrared: Geophysics., 42, 501-513
- Jensen, J.R. 2000, Remote Sensing of the Environment: An Earth source perspective. Prentice Hall. Upper Saddle River, NJ 1st Ed 444-528
- Kaye, C. A. 1959, Shoreline features and Quaternary shoreline changes, Puerto Rico, United State Geological Survey, U.S. Geological Survey Professional Paper 317-B

- Lee, Z.P., Carder, K.L., Hawes, S.K., Steward, R.G., Peacock, T.G., and Davis CO 1994. A model for interpretation of hyperspectral remote sensing reflectance. *Applied Optics*, 33: 5721-5732.
- Marsal, D. 1987, *Statistic for Geoscientists*, New York, USA Pergamon Press, 175 pp
- Morelock, J. 1978, *Shoreline of Puerto Rico: San Juan, PR: Coastal Zone Program*, Department of Natural Resources, 45p.
- Morelock, J. 2000, *Coastal Morphology & the Shoreline of Puerto Rico* webpage http://geology.uprm.edu/Morelock/GEOLOCN_/cstln.htm . Active May 2005
- Prothero, D.R. and Schwab. F. 1996 *Sedimentary Geology, Chapter 1 Sedimentary Rock: An Introduction* W. H. Freeman and Company. NY 6p
- Raymond, L.A 1994, *Sedimentary Rock. Petrology: The Study of Igneous, Sedimentary and Metamorphic Rocks*. McGraw Hill, 768p.
- Santiago, M., and Santiago-Rivera, L., 2000, *Hydrologic unit boundaries for the U.S. Virgin Islands: U.S. Geological Survey Open-File Report 99-223, 1CD.*
- Scofffin, T.P. 1987 *An Introduction to Carbonate Sediments and Rocks: Part 2 Carbonate Grains*. Chapman & Hall, NY p 15-60
- Trías, J.L, 1980 *Estudio estadístico de los parámetros físicos influyentes en la formación de las copas de dos playas de Puerto Rico*. Tesis M.S. Mayagüez Campus, University of Puerto Rico
- Tucker, M.E. and Wright, V.P 1990. *Carbonate Sedimentology*, Blackwell Science. Malden, MA 482 pp
- Vincent, R. K. 1997 *Geological and Environmental Remote Sensing*. Prentice Hall, Upper Saddle River, NJ, 357pp
- Watt, A. 1982, *Diccionario Ilustrado de la Geología*. Editorial Everest. León, España 208p
- Webb, R., Liboy, J., Hyman, L., Neal, W., Bush, D., and Pilkey, O., 1996, *Living with the Puerto Rico Shore*, Duke University Press, Durham, NC, United States 193pp.
- Zar, J. H. 1996. *Biostatistical Analysis*, Prentice Hall, Upper Saddle River, NJ 170p